

**UNCLASSIFIED**

**AD NUMBER**

**AD889893**

**LIMITATION CHANGES**

**TO:**

**Approved for public release; distribution is unlimited.**

**FROM:**

**Distribution authorized to U.S. Gov't. agencies only; Test and Evaluation; DEC 1971. Other requests shall be referred to Air Force Armament Laboratory, DLGC, Eglin AFB, FL 32542.**

**AUTHORITY**

**AFATL ltr, 24 Jun 1974**

**THIS PAGE IS UNCLASSIFIED**

AEDC-TR-71-261  
AFATL-TR-71-152

cy 2

DEC 29 1971

AUG 15 1985



# SEPARATION CHARACTERISTICS OF THE M-117 RETARDED BOMB, FINNED BLU-1C/B BOMB, AND SUU-42/A DISPENSER FROM THE A-7D AIRCRAFT AT MACH NUMBERS FROM 0.33 TO 0.95

David W. Hill, Jr.

ARO, Inc.

December 1971

This document contains neither recommendations nor conclusions of the Defense Department. Its distribution is unlimited. *Re TAB 74-17*  
*16 August 74*

Distribution limited to U.S. Government agencies only; this report contains information on test and evaluation of military hardware; December 1971; other requests for this document must be referred to Air Force Armament Laboratory (DLGC), Eglin AFB, Florida 32542.

**TECHNICAL REPORTS  
FILE COPY**

**PROPELLION WIND TUNNEL FACILITY  
ARNOLD ENGINEERING DEVELOPMENT CENTER  
AIR FORCE SYSTEMS COMMAND  
ARNOLD AIR FORCE STATION, TENNESSEE**

PROPERTY OF THE UNITED STATES  
AEDC  
F40600-76-C-0000

# **NOTICES**

When U. S. Government drawings, specifications, or other data are used for any purpose other than a definitely related Government procurement operation, the Government thereby incurs no responsibility nor any obligation whatsoever, and the fact that the Government may have formulated, furnished, or in any way supplied the said drawings, specifications, or other data, is not to be regarded by implication or otherwise, or in any manner licensing the holder or any other person or corporation, or conveying any rights or permission to manufacture, use, or sell any patented invention that may in any way be related thereto.

Qualified users may obtain copies of this report from the Defense Documentation Center.

References to named commercial products in this report are not to be considered in any sense as an endorsement of the product by the United States Air Force or the Government.

**SEPARATION CHARACTERISTICS OF THE  
M-117 RETARDED BOMB, FINNED BLU-1C/B BOMB,  
AND SUU-42/A DISPENSER FROM THE A-7D AIRCRAFT  
AT MACH NUMBERS FROM 0.33 TO 0.95**

**David W. Hill, Jr.  
ARO, Inc.**

This document has been approved for public release  
and its distribution is unlimited. *Per TAB 74-17  
H.S. 16 Aug; 74*

Distribution limited to U.S. Government agencies only;  
this report contains information on test and evaluation  
of military hardware; December 1971; other requests for  
this document must be referred to Air Force Armament  
Laboratory (DLGC), Eglin AFB, Florida 32542.

## FOREWORD

The work reported herein was sponsored by the Air Force Armament Laboratory (DLGC/Lt S. C. Braud), Armament Development and Test Center, Air Force Systems Command (AFSC), under Program Element 27121F, System 337A.

The test results presented were obtained by ARO, Inc. (a subsidiary of Sverdrup & Parcel and Associates, Inc.), contract operator of the Arnold Engineering Development Center (AEDC), AFSC, Arnold Air Force Station, Tennessee, under Contract F40600-72-C-0003. The test was conducted from September 11 through 16, 1971, under ARO Project No. PC0165. The manuscript was submitted for publication on November 4, 1971.

This technical report has been reviewed and is approved.

George F. Garey  
Lt Colonel, USAF  
AF Representative, PWT  
Directorate of Test

Duncan W. Rabey, Jr.  
Colonel, USAF  
Director of Test

## ABSTRACT

Tests were conducted in the Aerodynamic Wind Tunnel (4T) using 0.05-scale models to investigate the separation characteristics of the M-117 retarded bomb, finned BLU-1C/B bomb, and SUU-42/A dispenser when released from various wing pylon locations on the A-7D aircraft. Captive trajectory data were obtained at Mach numbers from 0.33 to 0.95 at simulated pressure altitudes from 4000 to 7000 ft. The parent-aircraft angle of attack was varied from 1.8 to 12.3 depending on Mach number, climb angle, and simulated altitude. At selected test conditions, parent climb angles of -70 deg were simulated. In general, for the trajectory intervals of the test, most of the stores separated from the parent aircraft without store-to-parent contact.

This document has been approved for public release  
its distribution is unlimited. *Per TAB 7413*  
*std 16 August 74*

Distribution limited to U.S. Government agencies only;  
this report contains information on test and evaluation  
of military hardware; December 1971; other requests for  
this document must be referred to Air Force Armament  
Laboratory (DLGC), Eglin AFB, Florida 32542.

## CONTENTS

|  | <u>Page</u> |
|--|-------------|
| <b>ABSTRACT</b> . . . . .  | iii         |
| <b>NOMENCLATURE</b> . . . . .  | vii         |
| <b>I. INTRODUCTION</b> . . . . .   | 1           |
| <b>II. APPARATUS</b> . . . . .   |             |
| 2.1 Test Facility . . . . .  | 1           |
| 2.2 Test Articles . . . . .  | 2           |
| 2.3 Instrumentation . . . . .  | 2           |
| <b>III. TEST DESCRIPTION</b> . . . . .                                       |             |
| 3.1 Test Conditions . . . . .  | 2           |
| 3.2 Data Acquisition . . . . .   | 3           |
| 3.3 Corrections . . . . .  | 3           |
| 3.4 Precision of Data . . . . .  | 4           |
| <b>IV. RESULTS AND DISCUSSION</b> . . . . .                                  |             |
| 4.1 General . . . . .  | 4           |
| 4.2 Trajectories for Various Store and Wing-Loading Configurations . . . . . | 4           |

## APPENDIXES

## I. ILLUSTRATIONS

Figure

|  |    |
|--|----|
| 1. Isometric Drawing of a Typical Store Separation Installation and a Block Diagram of the Computer Control Loop . . . . . | 9  |
| 2. Schematic of the Tunnel Test Section Showing Model Location . . . . .   | 10 |
| 3. Sketch of the A-7D Parent-Aircraft Model . . . . .  | 11 |
| 4. Details and Dimensions of the A-7D Model Pylons . . . . .   | 12 |
| 5. Details and Dimensions of the TER Model . . . . .   | 13 |
| 6. Details and Dimensions of the MER Model . . . . .   | 14 |
| 7. Details and Dimensions of the M-117R Model . . . . .  | 15 |
| 8. Details and Dimensions of the BLU-1C/B Unfinned Model . . . . .   | 16 |
| 9. Details and Dimensions of the BLU-1C/B Finned Model . . . . .   | 17 |
| 10. Details and Dimensions of the SUU-42/A Model . . . . .   | 18 |
| 11. Tunnel Installation Photograph Showing Parent Aircraft, Store, and CTS . . . . .                                       | 19 |
| 12. Schematic of the TER and MER Store Stations and Orientations . . . . .   | 20 |
| 13. Ejector Force Functions  |    |
| a. Function $T_1$ for M-117R on MER or TER . . . . .   | 21 |
| b. Function $T_2$ for BLU-1C/B on MAU-12 Pylon . . . . .   | 21 |
| c. Function $T_3$ for Empty SUU-42/A on MAU-12 Pylon . . . . .   | 22 |

| <u>Figure</u>   | <u>Page</u> |
|---|-------------|
| 14. Effect of Mach Number and Climb Angle on the Separation Trajectories<br>of the M-117R from Center Pylon Station, Inboard and Outboard<br>Pylon Empty                          |             |
| a. Configuration 1L . . . . .   | 23          |
| b. Configuration 2L . . . . .   | 24          |
| c. Configuration 3L . . . . .   | 25          |
| d. Configuration 4L . . . . .   | 26          |
| e. Configuration 5L . . . . .   | 27          |
| f. Configuration 6R . . . . .   | 28          |
| g. Configuration 7R . . . . .   | 29          |
| 15. Effect of Mach Number and Climb Angle on the Separation Trajectories<br>of the M-117R from Center Pylon Station, Finned BLU-1C/B on Inboard<br>and Outboard Pylon             |             |
| a. Configuration 8R . . . . .   | 30          |
| b. Configuration 9R . . . . .   | 31          |
| c. Configuration 10R . . . . .  | 32          |
| d. Configuration 11R . . . . .  | 33          |
| e. Configuration 12R . . . . .  | 34          |
| 16. Effect of Mach Number on the Separation Trajectories of M-117R from<br>Center Pylon Station, Outboard Pylon Empty, and M-117R on Inboard<br>Pylon                             |             |
| a. Configuration 13R . . . . .  | 35          |
| b. Configuration 14R . . . . .  | 36          |
| c. Configuration 15R . . . . .  | 37          |
| d. Configuration 16R . . . . .  | 38          |
| e. Configuration 17R . . . . .  | 39          |
| f. Configuration 18R . . . . .  | 40          |
| 17. Effect of Mach Number on the Separation Trajectories of the M-117R<br>from Center Pylon Station, Unfinned BLU-1C/B on Outboard and Inboard<br>Pylons                          |             |
| a. Configuration 19L . . . . .  | 41          |
| b. Configuration 20L . . . . .  | 42          |
| 18. Effect of Mach Number on the Separation Trajectories of the M-117R from<br>Center Pylon Station, M-117R on Inboard, and SUU-42/A on Outboard<br>Pylon                         |             |
| a. Configuration 21L . . . . .  | 43          |
| b. Configuration 22L . . . . .  | 44          |
| c. Configuration 23L . . . . .  | 45          |
| d. Configuration 24L . . . . .  | 46          |
| e. Configuration 25L . . . . .  | 47          |
| f. Configuration 26L . . . . .  | 48          |
| 19. Effect of Mach Number on the Separation Trajectories of the SUU-42/A<br>from the Outboard Pylon, MER on Center Pylon, and Inboard Pylon<br>Empty, Configuration 27R . . . . . | 49          |

| <u>Figure</u>  | <u>Page</u> |
|--|-------------|
| 20. Effect of Mach Number on the Separation Trajectories of the SUU-42/A from the Outboard Pylon, MER with M-117R on Center Pylon, and an M-117R on Inboard Pylon, Configuration 28L . . . . . | 50          |
| 21. Effect of Mach Number and Climb Angle on the Separation Trajectories of the Finned BLU-1C/B from the Inboard Pylon, MER on Center Pylon, and Finned BLU-1C/B on Outboard Pylon             |             |
| a. Configuration 29L . . . . .   | 51          |
| b. Configuration 30R . . . . .   | 52          |

## II. TABLES

|  |    |
|--|----|
| I. Full-Scale Store Parameters Used in Trajectory Calculations . . . . .               | 53 |
| II. Maximum Full-Scale Position Uncertainties Caused by Balance Inaccuracies . . . . . | 54 |
| III. Aircraft Wing-Loading Configuration . . . . .                                     | 55 |

## NOMENCLATURE

|                                  |  |
|----------------------------------|--|
| <b>BL</b>                        | Aircraft buttock line from plane of symmetry, in., model scale                                   |
| <b>b</b>                         | Store reference dimension, 1.688 ft, full scale  |
| <b>C<sub>m</sub></b>             | Store pitching-moment-coefficient, referenced to the store cg, pitching moment/ $q_{\infty} S_b$ |
| <b>C<sub>m<sub>q</sub></sub></b> | Store pitch-damping derivative, $dC_m/d(qb/2V_{\infty})$   |
| <b>C<sub>n</sub></b>             | Store yawing-moment coefficient, referenced to the store cg, yawing moment/ $q_{\infty} S_b$     |
| <b>C<sub>n<sub>r</sub></sub></b> | Store yaw-damping derivative, $dC_n/d(rb/2V_{\infty})$   |
| <b>F<sub>Z</sub></b>             | MER/TER ejector force, lb  |
| <b>F<sub>Z<sub>1</sub></sub></b> | Pylon forward ejector force, lb  |
| <b>F<sub>Z<sub>2</sub></sub></b> | Pylon aft ejector force, -lb   |
| <b>H</b>                         | Pressure altitude, ft  |
| <b>I<sub>yy</sub></b>            | Full-scale moment of inertia about the store Y <sub>B</sub> axis, slug-ft <sup>2</sup>           |
| <b>I<sub>zz</sub></b>            | Full-scale moment of inertia about the store Z <sub>B</sub> axis, slug-ft <sup>2</sup>           |

|            |   |
|------------|---|
| $M_\infty$ | Free-stream Mach number   |
| $\bar{m}$  | Full-scale store mass, slugs  |
| $p_\infty$ | Free-stream static pressure, psfa   |
| $q$        | Store angular velocity about the $Y_B$ axis, radians/sec  |
| $q_\infty$ | Free-stream dynamic pressure, psf   |
| $r$        | Store angular velocity about the $Z_B$ axis, radians/sec  |
| $S$        | Store reference area, $\text{ft}^2$ , full scale  |
| $t$        | Real trajectory time from initiation of trajectory, sec   |
| $V_\infty$ | Free-stream velocity, ft/sec  |
| WL         | Aircraft waterline from reference horizontal plane, in., model scale  |
| X          | Separation distance of the store cg parallel to the flight axis system $X_F$ direction, ft, full scale measured from the prelaunch position       |
| $X_{cg}$   | Full-scale cg location, ft, from nose of store  |
| $X_L$      | Ejector piston location relative to the store cg, positive forward of store cg, ft, full scale  |
| $X_{L_1}$  | Forward ejector piston location relative to the store cg, positive forward of store cg, ft, full scale  |
| $X_{L_2}$  | Aft ejector piston location relative to the store cg, positive forward of store cg, ft, full scale  |
| Y          | Separation distance of the store cg parallel to the flight axis system $Y_F$ direction, ft, full scale measured from the prelaunch position       |
| Z          | Separation distance of the store cg parallel to the flight-axis system $Z_F$ direction, ft, full scale measured from the prelaunch position       |
| ZE         | Ejector stroke length, ft, full scale   |
| $\alpha$   | Parent-aircraft model angle of attack relative to the free-stream velocity vector, deg  |
| $\theta$   | Angle between the store longitudinal axis and its projection in the $X_F$ - $Y_F$ plane, positive when store nose is raised as seen by pilot, deg |

- $\bar{\theta}$  Simulated parent-aircraft climb angle. Angle between the flight direction and the earth horizontal, deg, positive for increasing altitude
- $\psi$  Angle between the projection of the store longitudinal axis in the  $X_F$ - $Y_F$  plane and the  $X_F$  axis, positive when the store nose is to the right as seen by the pilot, deg
- $\phi$  Angle between the projection of the store lateral axis in the  $Y_F$ - $Z_F$  plane and the  $Y_F$  axis, positive for clockwise rotation when looking upstream, deg

## FLIGHT-AXIS SYSTEM COORDINATES

### Directions

- $X_F$  Parallel to the free-stream wind vector, positive direction is forward as seen by the pilot
- $Y_F$  Perpendicular to the  $X_F$  and  $Z_F$  directions, positive direction is to the right as seen by the pilot
- $Z_F$  In the aircraft plane of symmetry, perpendicular to the free-stream wind vector, positive direction is downward

The flight-axis system origin is coincident with the aircraft cg and remains fixed with respect to the parent aircraft during store separation. The  $X_F$ ,  $Y_F$ , and  $Z_F$  coordinate axes do not rotate with respect to the initial flight direction and attitude.

## STORE BODY-AXIS SYSTEM COORDINATES

### Directions

- $X_B$  Parallel to the store longitudinal axis, positive direction is upstream in the prelaunch position
- $Y_B$  Perpendicular to the store longitudinal axis, and parallel to the flight-axis system  $X_F$ - $Y_F$  plane when the store is at zero roll angle, positive direction is to the right looking upstream when the store is at zero yaw and roll angles
- $Z_B$  Perpendicular to both the  $X_B$  and  $Y_B$  axes, positive direction is downward as seen by the pilot when the store is at zero pitch and roll angles.

The store body-axis system origin is coincident with the store cg and moves with the store during separation from the parent airplane. The  $X_B$ ,  $Y_B$ , and  $Z_B$  coordinate axes rotate with the store in pitch, yaw, and roll so that mass moments of inertia about the three axes are not time-varying quantities.

## SECTION I INTRODUCTION

A captive trajectory test was conducted in the Aerodynamic Wind Tunnel (4T), Propulsion Wind Tunnel Facility, to determine the separation characteristics of the M-117R bomb, finned BLU-1C/B bombs, and a SUU-42/A dispenser. Separation trajectories were initiated from the carriage position with simulated ejector forces acting on the stores.

To determine the separation trajectories, 0.05-scale models of the A-7D aircraft and various stores were employed. The flight conditions simulated were Mach numbers from 0.33 to 0.95 and altitudes from 4000 to 7000 ft. At selected test conditions, parent-aircraft climb angles of 0 and -70 deg were simulated. The separation trajectories were initiated from various wing pylon locations on the parent aircraft. The ejector forces used were time-variant functions provided by the Air Force Armament Laboratory (AFATL).

## SECTION II APPARATUS

### 2.1 TEST FACILITY

The Aerodynamic Wind Tunnel (4T) is a closed-loop, continuous flow, variable density tunnel in which the Mach number can be varied from 0.1 to 1.3. At all Mach numbers, the stagnation pressure can be varied from 300 to 3700 psfa. The test section is 4 ft square and 12.5 ft long with perforated, variable porosity (0.5- to 10-percent open) walls. It is completely enclosed in a plenum chamber from which the air can be evacuated, allowing part of the tunnel airflow to be removed through the perforated walls of the test section.

For store separation testing, two separate and independent support systems are used to support the models. The parent-aircraft model is inverted in the test section and supported by an offset sting attached to the main pitch sector. The store model is supported by the captive trajectory support (CTS) which extends down from the tunnel top wall and provides store movement (six degrees of freedom) independent of the parent-aircraft model. An isometric drawing of a typical store separation installation is shown in Fig. 1, Appendix I.

Also shown in Fig. 1 is a block diagram of the computer control loop used during captive trajectory testing. The analog system and the digital computer work as an integrated unit and, utilizing required input information, control the store movement during a trajectory. Store positioning is accomplished by use of six individual d-c electric motors. Maximum translational travel of the CTS is  $\pm 15$  in. from the tunnel centerline in the lateral and vertical directions and 36 in. in the axial direction. Maximum angular displacements are  $\pm 45$  deg in pitch and yaw and  $\pm 360$  deg in roll. A more complete description of the test facility can be found in the Test Facilities Handbook.<sup>1</sup> A schematic

---

<sup>1</sup>Test Facilities Handbook (Ninth Edition). "Propulsion Wind Tunnel Facility. Vol. 4." Arnold Engineering Development Center, July 1971.

showing the test section details and the location of the models in the tunnel is shown in Fig. 2.

## 2.2 TEST ARTICLES

The test articles were 0.05-scale models of the A-7D parent aircraft and the various stores. A sketch showing the basic dimensions of the A-7D parent model is shown in Fig. 3. Details and dimensions of the pylons, Multiple Ejection Rack (MER), and Triple Ejection Rack (TER) are shown in Figs. 4, 5, and 6, and the store models are shown in Figs. 7 through 10.

The A-7D parent model was geometrically similar to the full-scale airplane except for some modifications incident to the wind-tunnel installation and CTS operation. Horizontal tail surfaces were removed because of interference with the CTS support. The parent model was inverted in the tunnel and attached by a 23-deg offset sting to the main sting support system (Fig. 2). Figure 11 shows a typical tunnel installation photograph of the parent aircraft and store model.

The A-7D aircraft has three pylon stations on each wing. The mounting surfaces of all three pylons are inclined at a 3.0-deg nose-down angle with respect to the aircraft waterline.

The store models were mounted on an internal balance which was an integral part of a 30-deg offset sting. The sting was in turn connected to the CTS support (Figs. 2 and 11).

## 2.3 INSTRUMENTATION

A five-component, internal strain-gage balance was used to obtain the force and moment data on the store models. Translational and angular positions of the store models were obtained from the CTS analog outputs. The parent-aircraft angle of attack was set using an absolute angle-of-attack indicator located in the nose of the parent model. The CTS was electrically connected to automatically stop and give a visual indication if the store model or sting contacted the parent-aircraft surface. Spring-loaded plungers were located in the pylons, MER, and TER in order to provide a position indication when the store model was in the launch position. The plunger circuit was independent of the parent-aircraft grounding circuit.

## SECTION III TEST DESCRIPTION

### 3.1 TEST CONDITIONS

Separation trajectory data were obtained at Mach numbers from 0.33 to 0.95. Tunnel dynamic pressure ranged from 250 psf at  $M_\infty = 0.33$  to 500 psf at  $M_\infty = 0.95$ , and tunnel stagnation temperature was maintained near 110°F.

Tunnel conditions were held constant at the desired Mach number and stagnation pressure while data for each trajectory were obtained. The trajectories were terminated when the store or sting contacted the parent-aircraft model or when a CTS tunnel limit was reached.

### 3.2 DATA ACQUISITION

To obtain a trajectory, test conditions were established in the tunnel and the parent model was positioned at the desired angle of attack. The store model was then oriented to a position corresponding to the store carriage location. After the store was set at the desired initial position, operational control of the CTS was switched to the digital computer which controlled the store movement during the trajectory through commands to the CTS analog system (see block diagram, Fig. 1). Data from the wind tunnel, consisting of measured model forces and moments, wind-tunnel operating conditions, and CTS positions, were input to the digital computer for use in the full-scale trajectory calculations.

The digital computer was programmed to solve the six-degree-of-freedom equations to calculate the angular and linear displacements of the store relative to the parent-aircraft pylon. In general, the program involves using the last two successive measured values of each static aerodynamic coefficient to predict the magnitude of the coefficients over the next time interval of the trajectory. These predicted values are used to calculate the new position and attitude of the store at the end of the time interval. The CTS is then commanded to move the store model to this new position and the aerodynamic loads are measured. If these new measurements agree with the predicted values, the process is continued over another time interval of the same magnitude. If the measured and predicted values do not agree within the desired precision, the calculation is repeated over a time interval one-half the previous value. This process is repeated until a complete trajectory has been obtained.

In applying the wind-tunnel data to the calculations of the full-scale store trajectories, the measured forces and moments are reduced to coefficient form and then applied with proper full-scale store dimensions and flight dynamic pressure. Dynamic pressure was calculated using a flight velocity equal to the free-stream velocity component plus the components of store velocity relative to the aircraft, and a density corresponding to the simulated altitude.

The initial portion of each trajectory from the carriage position incorporated simulated ejector forces in addition to the measured aerodynamic forces acting on the store. The ejector force functions for the stores are presented in Fig. 13. The ejector force was considered to act perpendicular to the rack or pylon mounting surface. The locations of the applied ejector forces and other full-scale store parameters used in the trajectory calculations are listed in Table I, Appendix II.

### 3.3 CORRECTIONS

Balance, sting, and support deflections caused by the aerodynamic loads on the store models were accounted for in the data reduction program to calculate the true store-model

angles. Corrections were also made for model weight tares to calculate the net aerodynamic forces on the store model.

### 3.4 PRECISION OF DATA

The trajectory data are subject to error from several sources including tunnel conditions, balance measurements, extrapolation tolerances allowed in the predicted coefficients, computer inputs, and CTS positioning control. Maximum error in the CTS position control was  $\pm 0.05$  in. for the translational settings and  $\pm 0.15$  deg for angular displacement settings in pitch and yaw. Extrapolation tolerances were  $\pm 0.10$  for each of the aerodynamic coefficients. The maximum uncertainties in the full-scale position data caused by the balance precision limitations are given in Table II. The estimated uncertainty in setting Mach number was no greater than  $\pm 0.003$ , and the uncertainty in parent-model angle of attack was estimated to be  $\pm 0.1$  deg.

## SECTION IV RESULTS AND DISCUSSION

### 4.1 GENERAL

The data presented herein were obtained to show the effects of wing-loading configuration and Mach number on the separation trajectories of the M-117R bomb, finned BLU-1C/B bomb, and the SUU-42/A dispenser. The time variant ejector forces and store parameters shown in Fig. 13 and Table I, respectively, were used in determining the trajectories.

In the trajectory data, the full-scale linear and angular displacements of the store relative to the carriage positions on the rack or pylon are presented versus full-scale trajectory time.

Table III describes the wing-loading configurations used in the data presentation. The L or R notation for each configuration number denotes left or right wing, respectively.

### 4.2 TRAJECTORIES FOR VARIOUS STORE AND WING-LOADING CONFIGURATIONS

Figures 14 through 18 show the effect of Mach number and climb angle on trajectories for the M-117R store released from the center pylon station. The M-117R was released at various stations on the MER or TER with the inboard and outboard pylons empty (Fig. 14), with dummy finned BLU-1C/B stores on the inboard and outboard pylons (Fig. 17), and with a dummy M-117R on the inboard pylon and a SUU-42/A on the outboard pylon (Fig. 18).

Figures 19 and 20 show the effect of Mach number on the separation trajectories of the SUU-42/A from the outboard pylon. Figure 21 shows the effect of Mach number and climb angle on the separation trajectories of the finned BLU-1C/B from the inboard pylon.

In general, for the trajectory intervals of this test, most of the stores separated from the parent aircraft without store-to-parent contact. A few of the trajectories were terminated as a result of reaching the vertical travel limit of the CTS or contact of the store-model-support sting with the parent-aircraft model.

**APPENDIXES**

- I. ILLUSTRATIONS**
- II. TABLES**

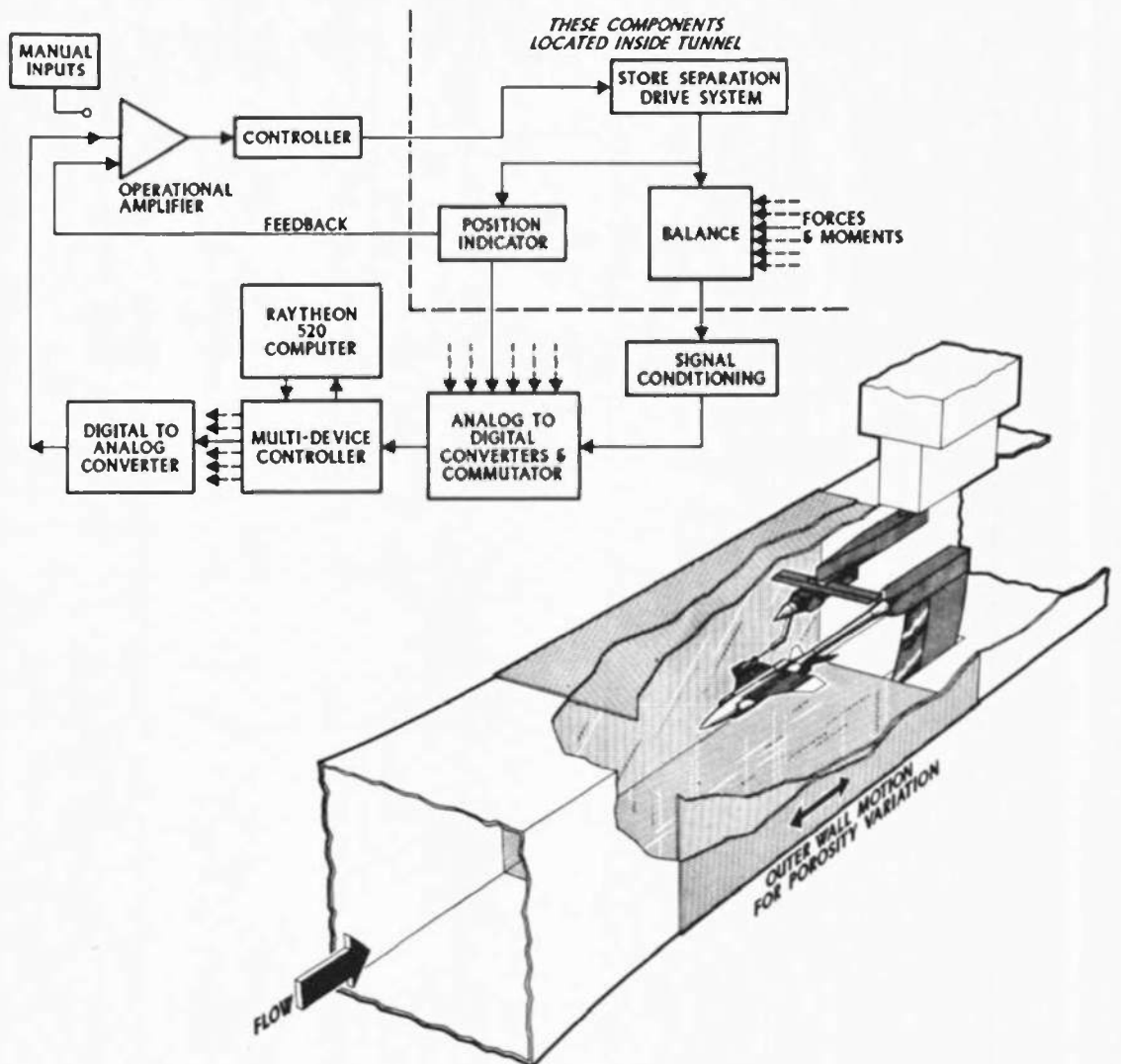


Fig. 1 Isometric Drawing of a Typical Store Separation Installation and a Block Diagram of the Computer Control Loop

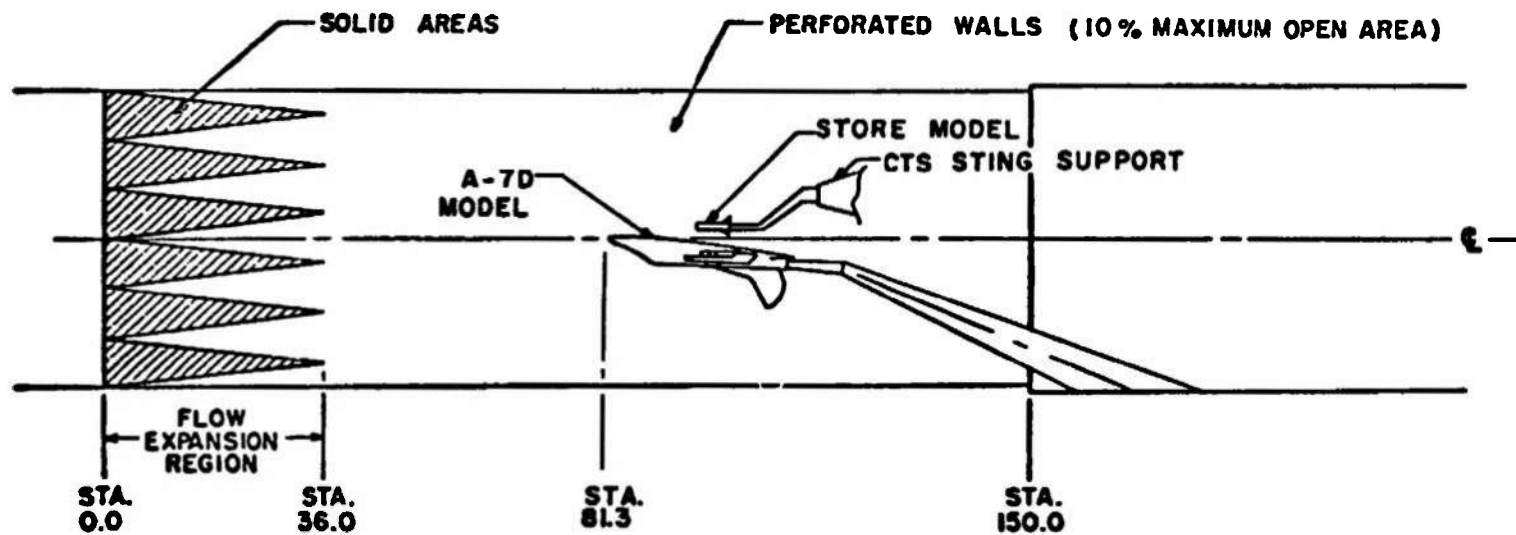
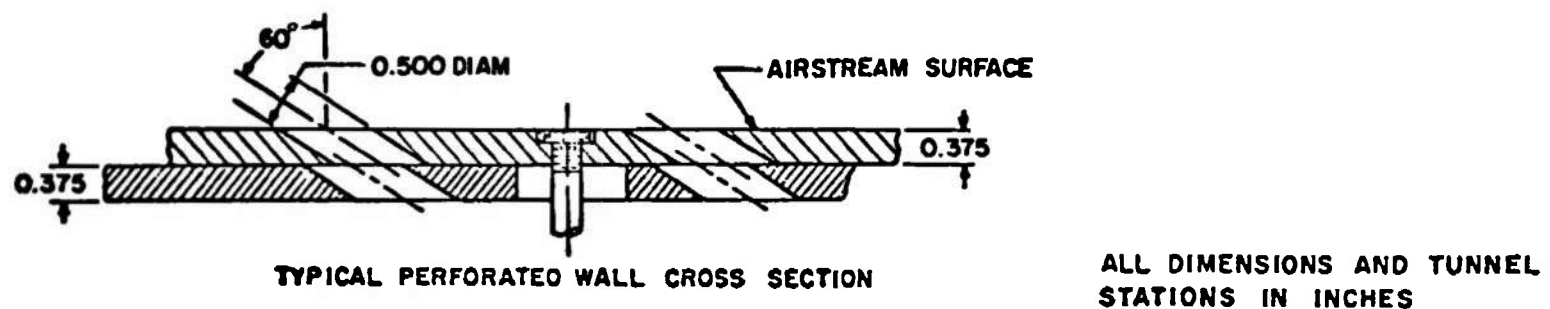


Fig. 2 Schematic of the Tunnel Test Section Showing Model Location

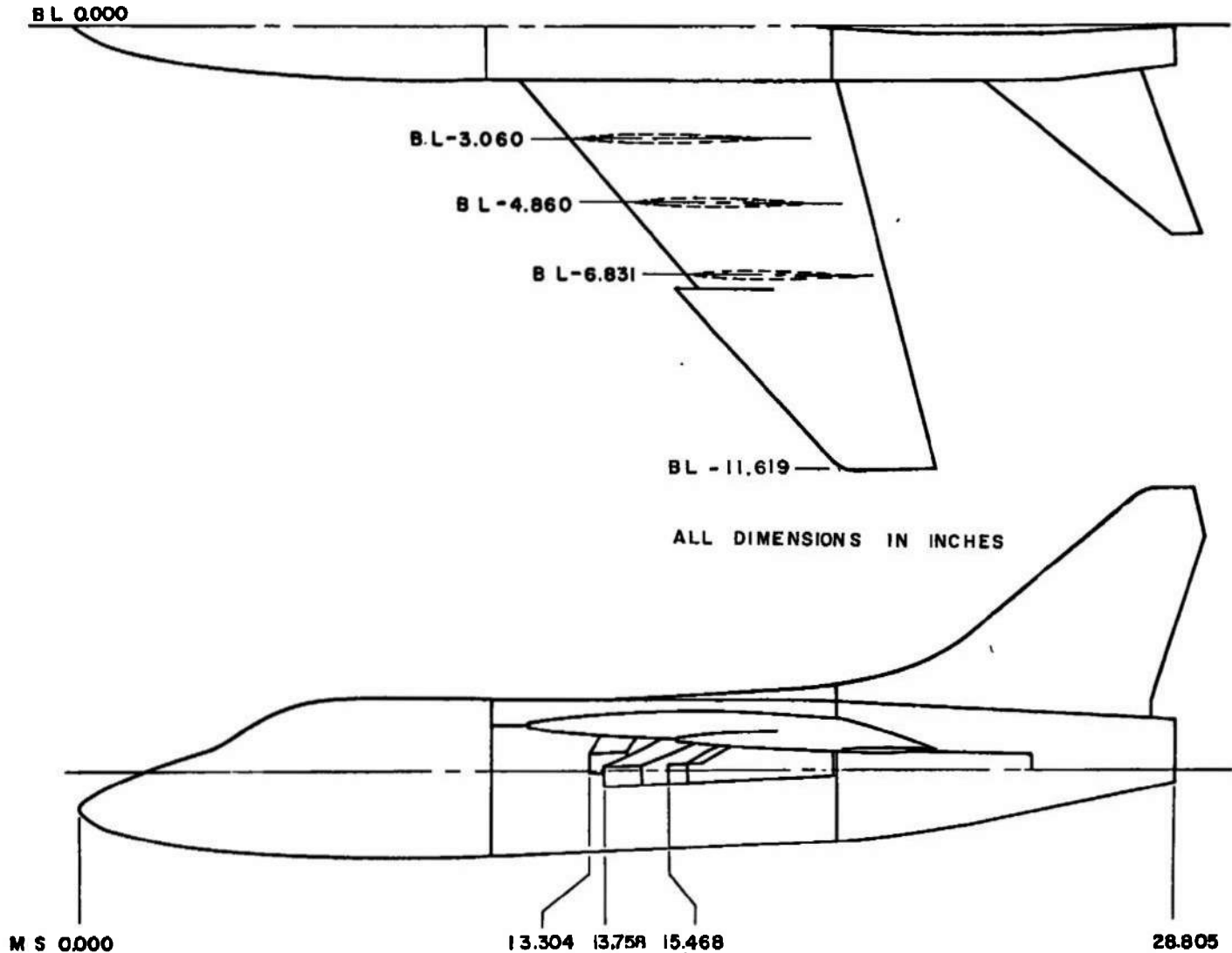
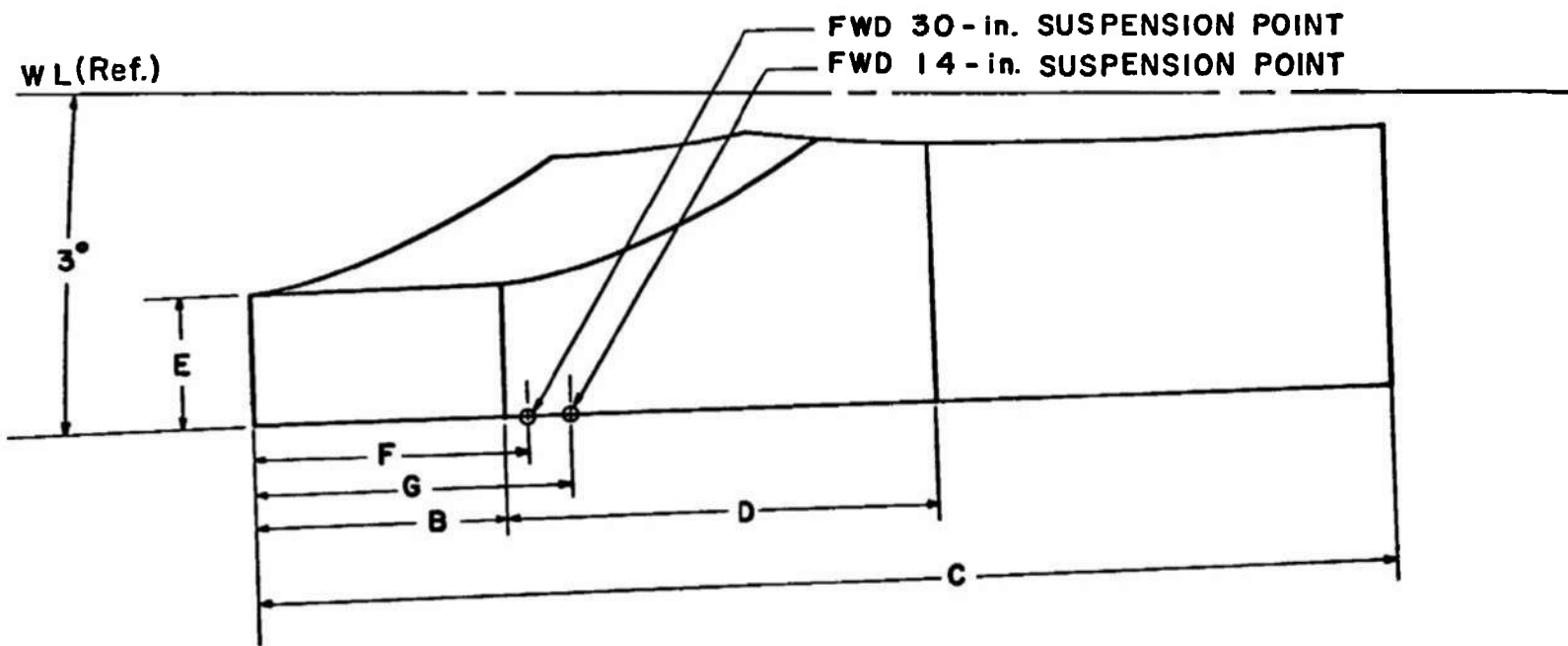


Fig. 3 Sketch of the A-7D Parent-Aircraft Model



|   | INBOARD | CENTER | OUTBOARD |
|---|---------|--------|----------|
| B | 1.030   | 1.030  | 0.515    |
| C | 4.580   | 4.850  | 4.437    |
| D | 1.630   | 1.905  | 2.008    |
| E | 0.575   | 0.575  | 0.513    |
| F | 0.950   | 0.950  | 0.750    |
| G | 1.350   | 1.350  | 1.150    |

ALL DIMENSIONS IN INCHES

Fig. 4 Details and Dimensions of the A-7D Model Pylons

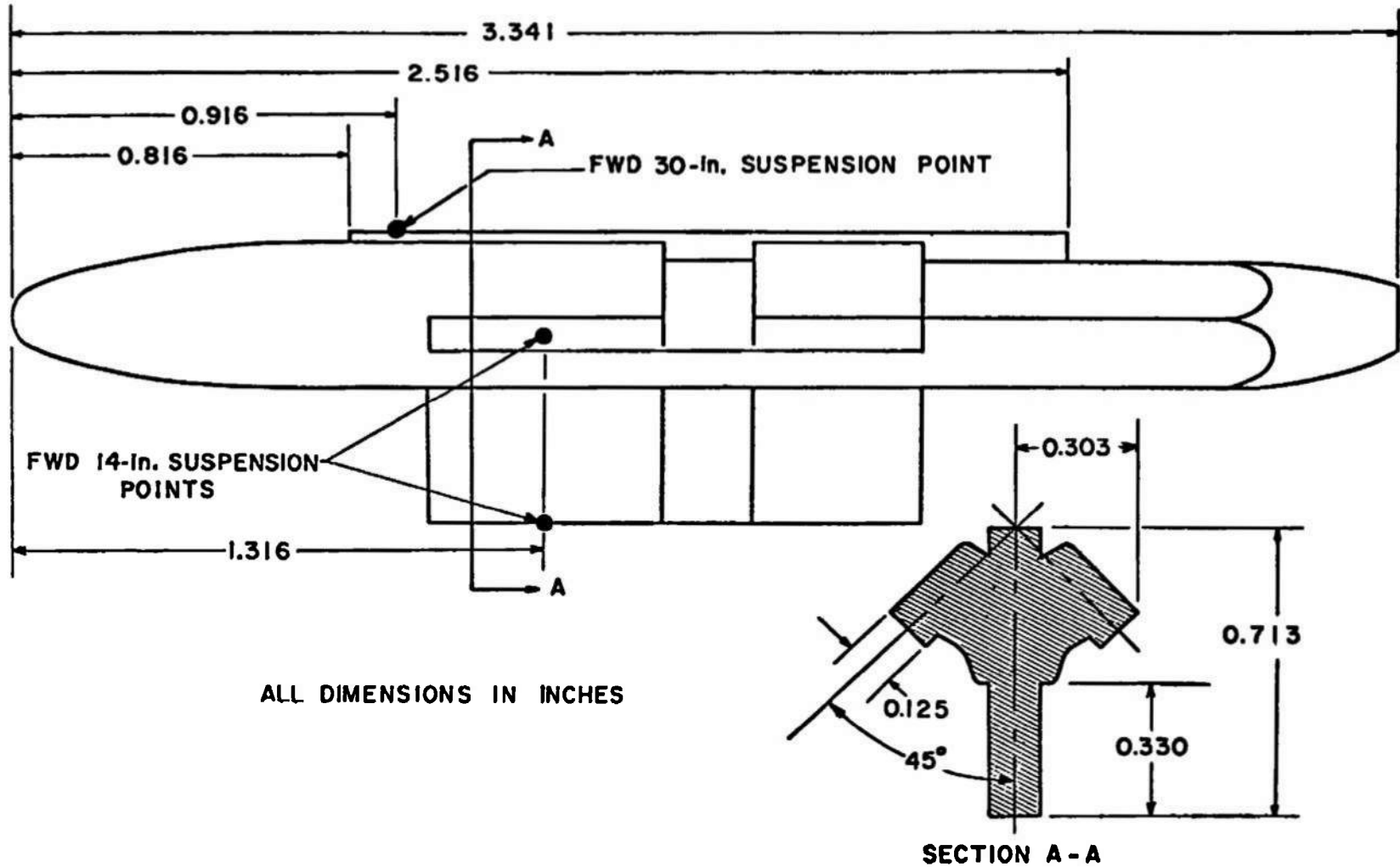


Fig. 5 Details and Dimensions of the TER Model

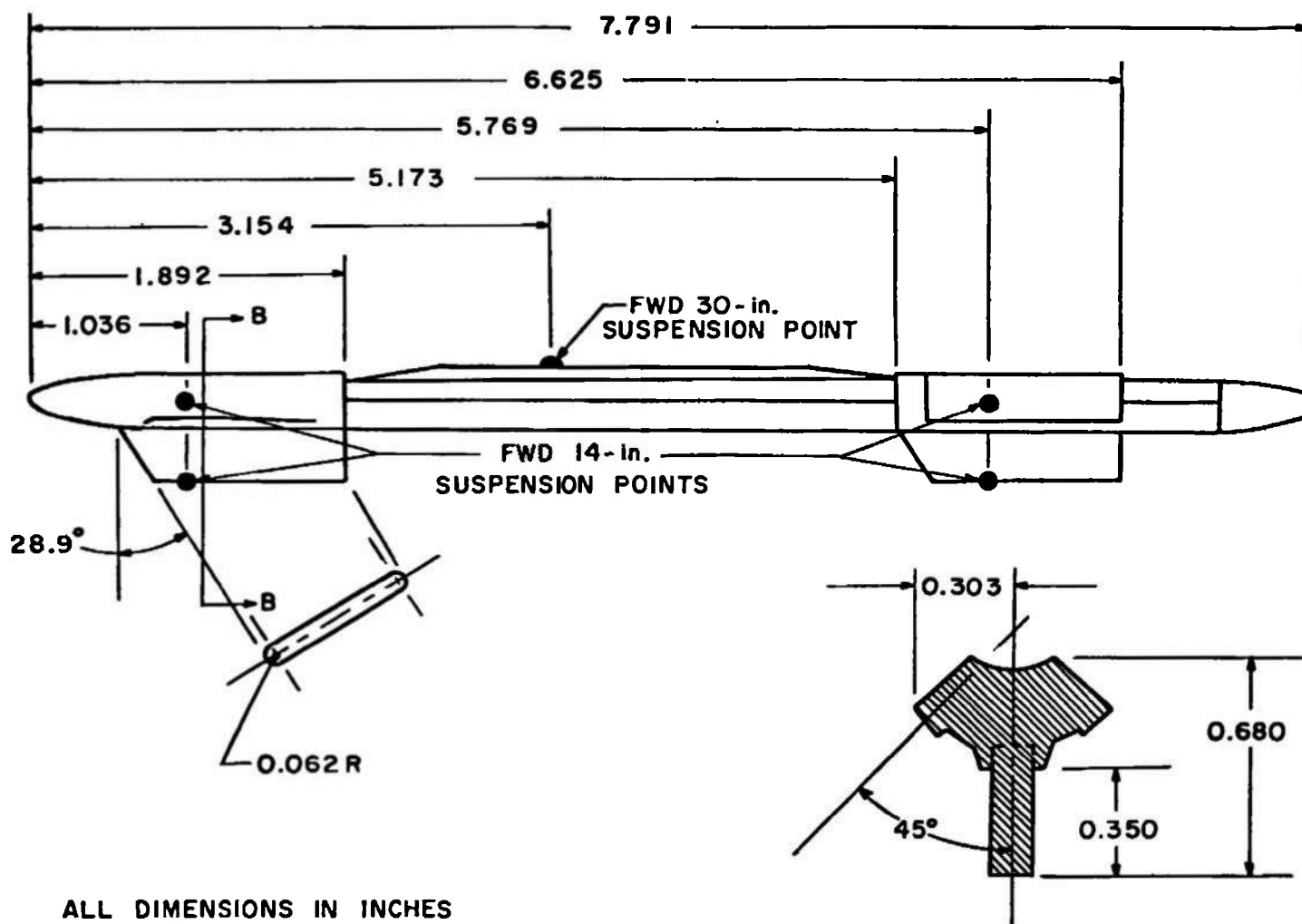


Fig. 6 Details and Dimensions of the MER Model

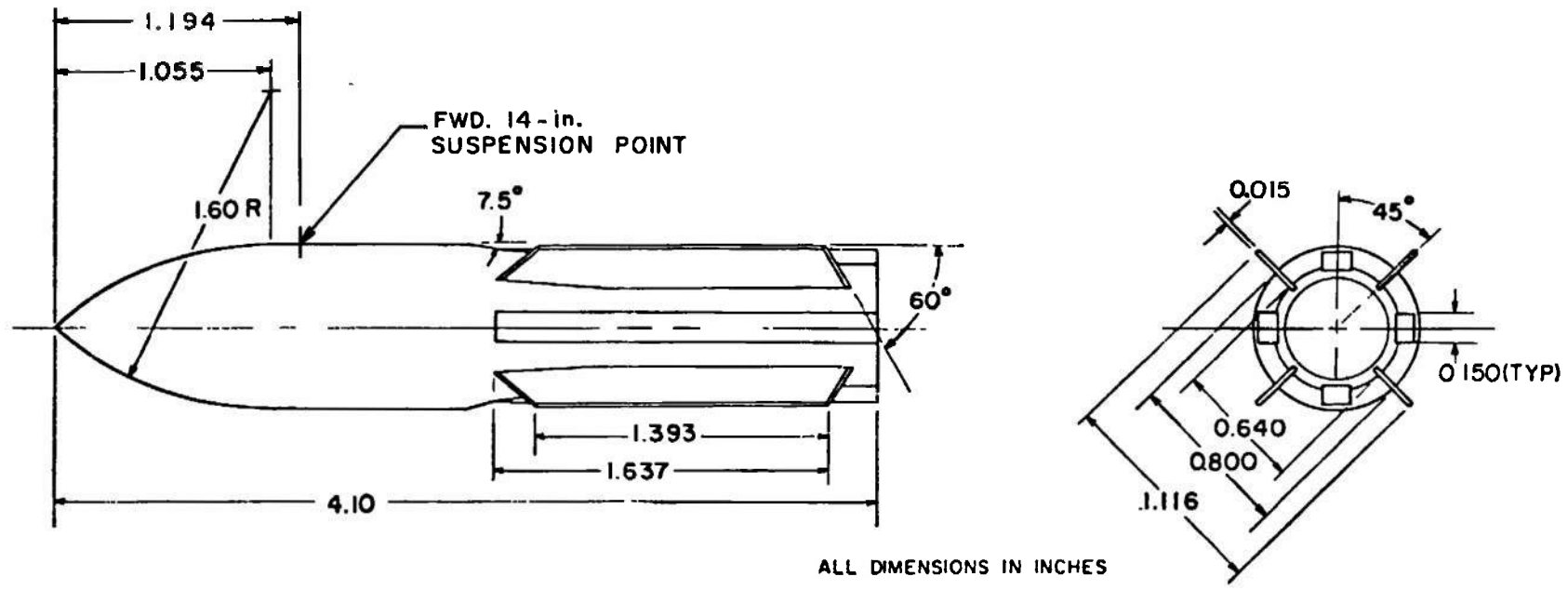


Fig. 7 Details and Dimensions of the M-117R Model

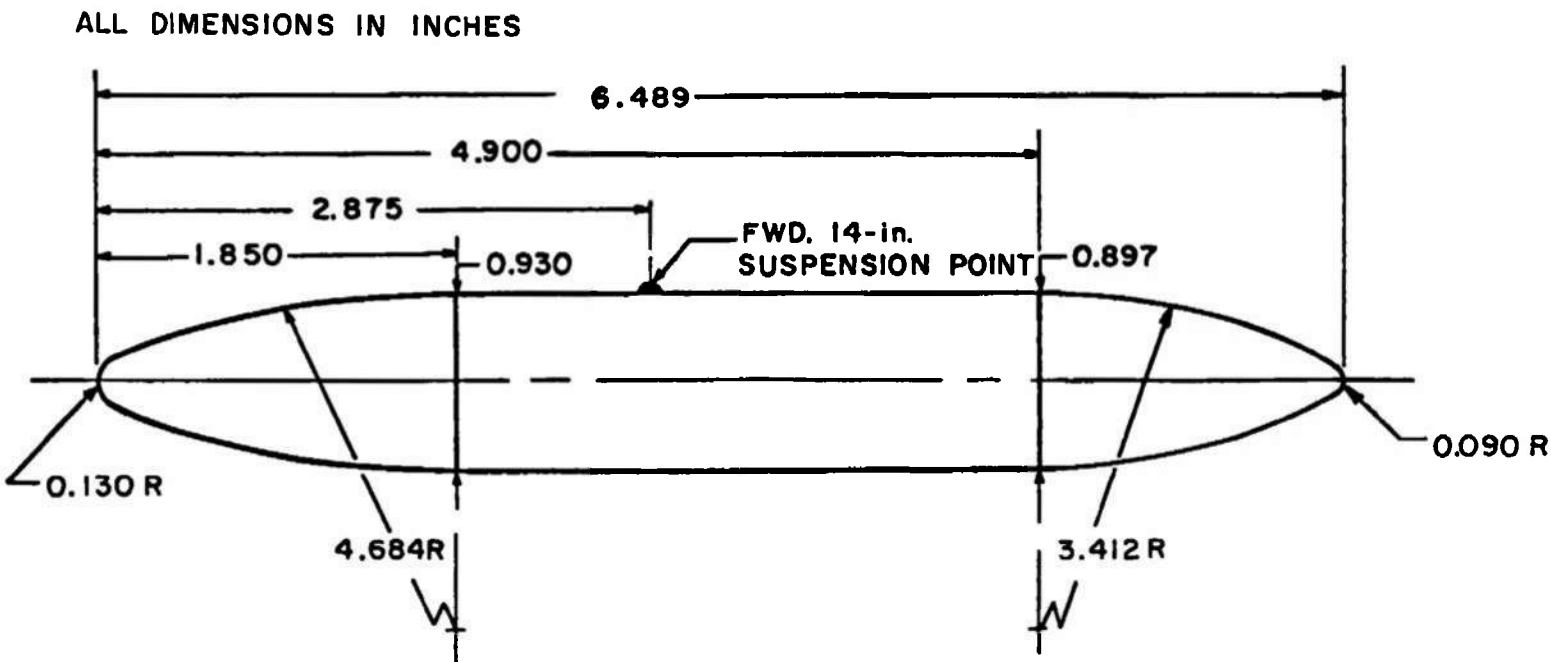


Fig. 8 Details and Dimensions of the BLU-1C/B Unfinned Model

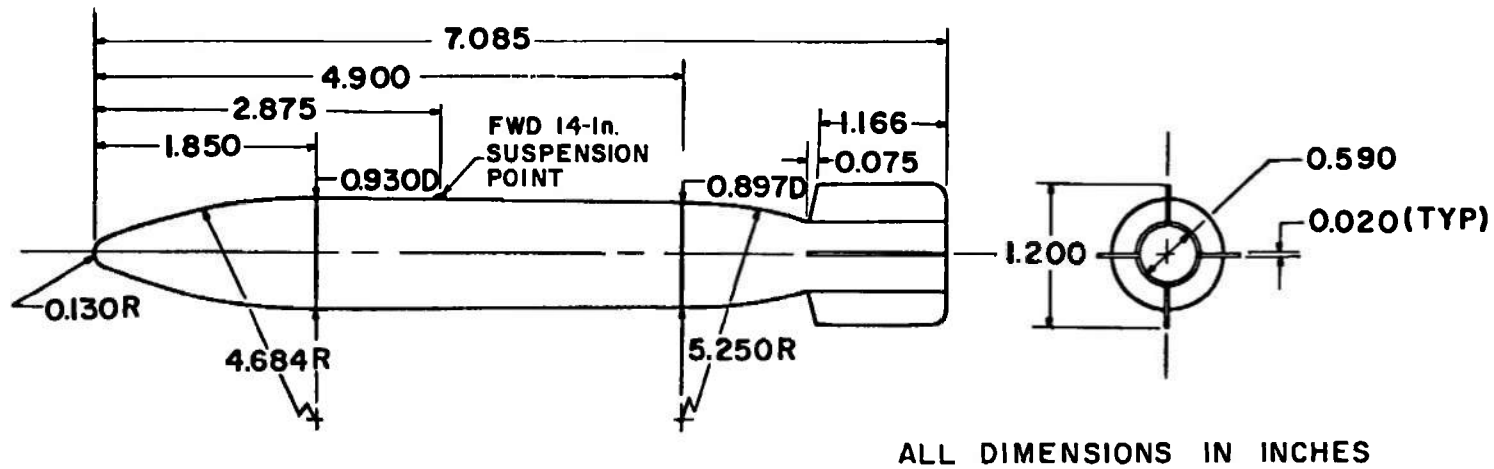


Fig. 9 Details and Dimensions of the BLU-1C/B Finned Model

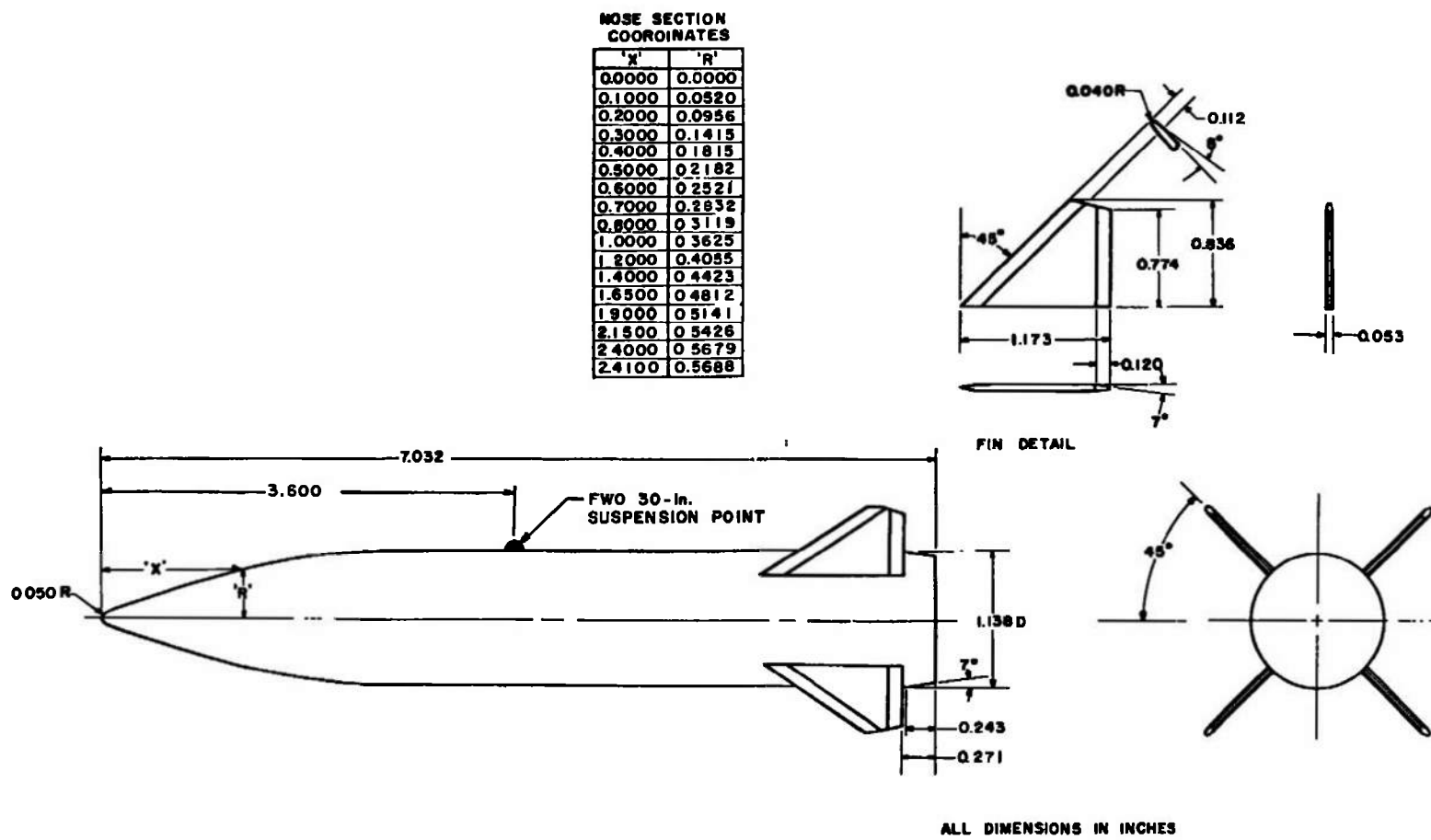


Fig. 10 Details and Dimensions of the SUU-42/A Model

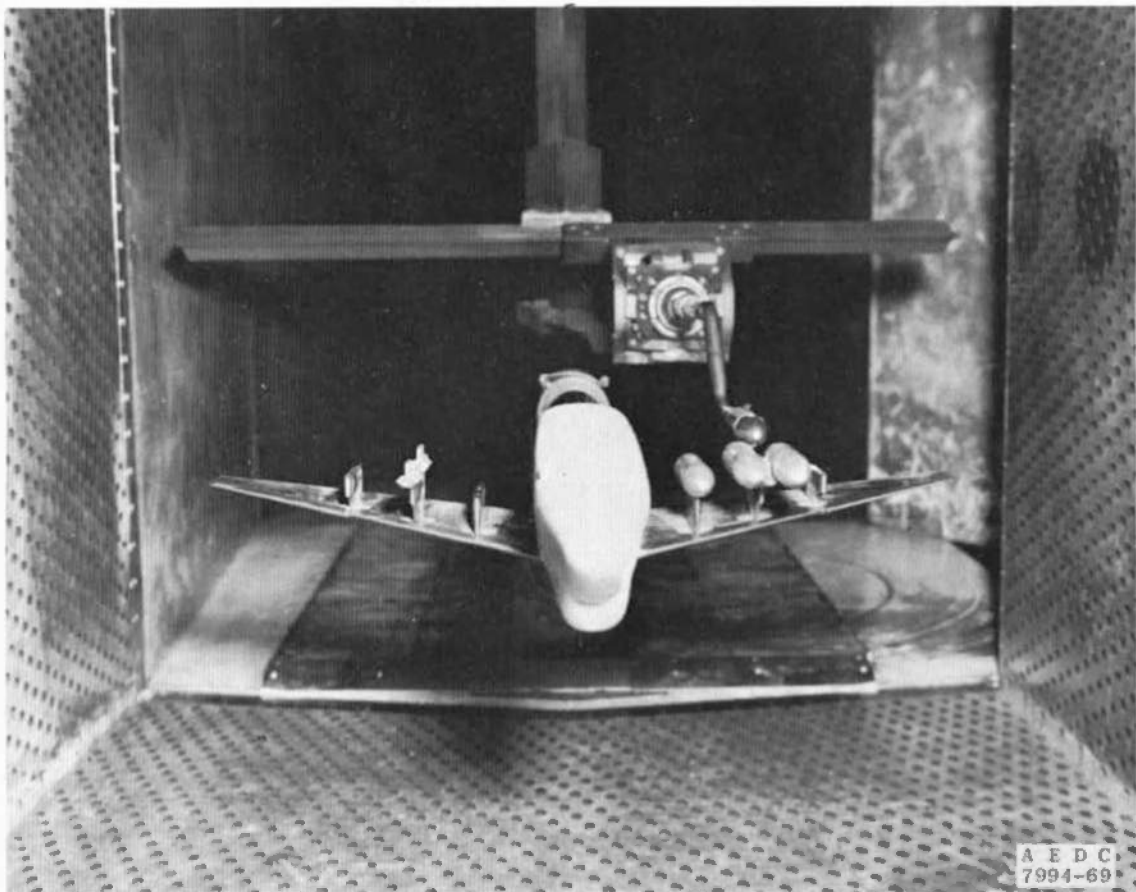
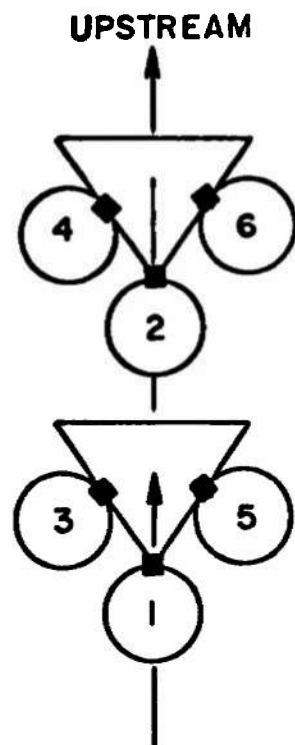
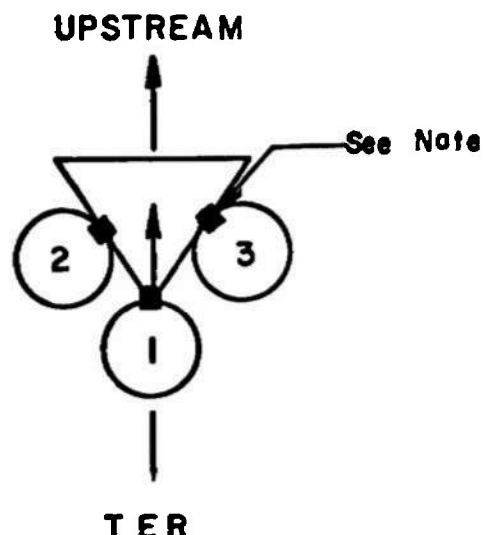


Fig. 11 Tunnel Installation Photograph Showing Parent Aircraft, Store, and CTS



MER

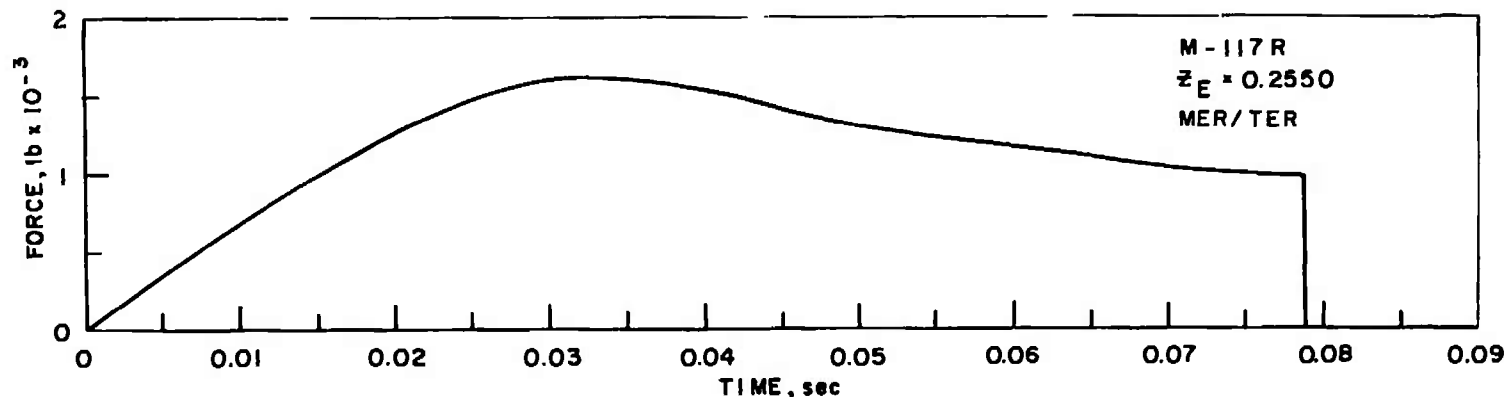


TER

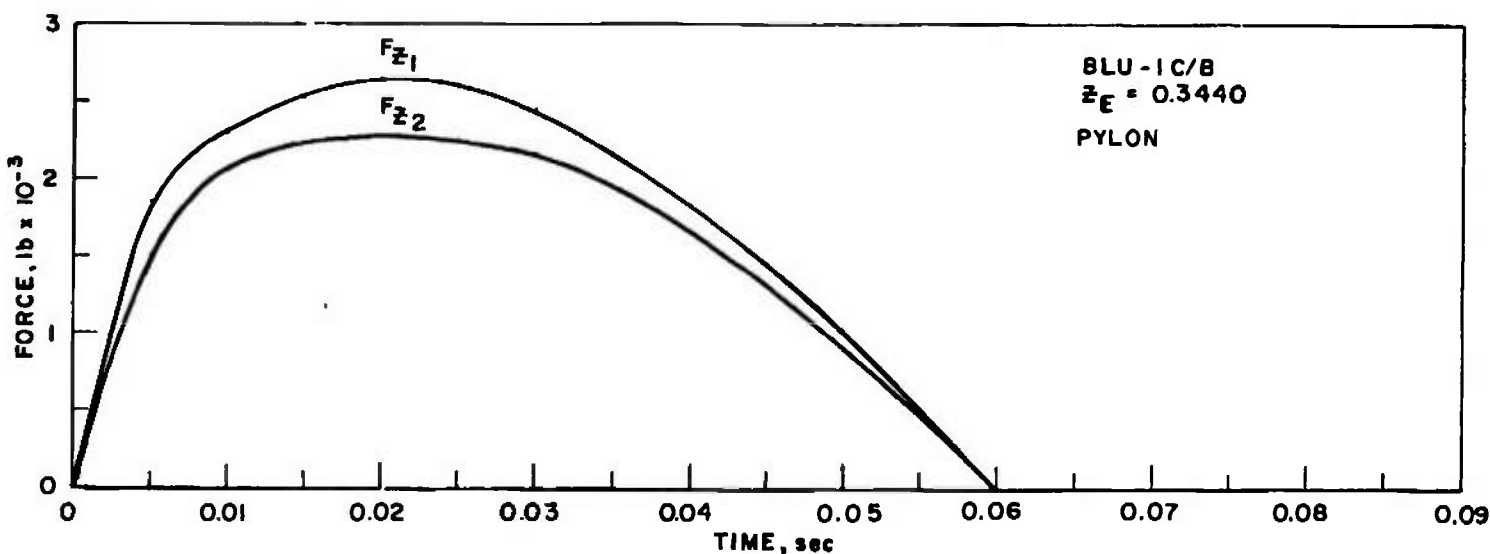
**NOTE:** The square indicates the orientation of the suspension lugs.

| TYPE<br>RACK | STATION | ROLL<br>ORIENTATION, deg |
|--------------|---------|--------------------------|
| MER          | 1       | 0                        |
|              | 2       | 0                        |
|              | 3       | 45                       |
|              | 4       | 45                       |
|              | 5       | -45                      |
|              | 6       | -45                      |
| TER          | 1       | 0                        |
|              | 2       | 45                       |
|              | 3       | -45                      |

Fig. 12 Schematic of the TER and MER Store Stations and Orientations

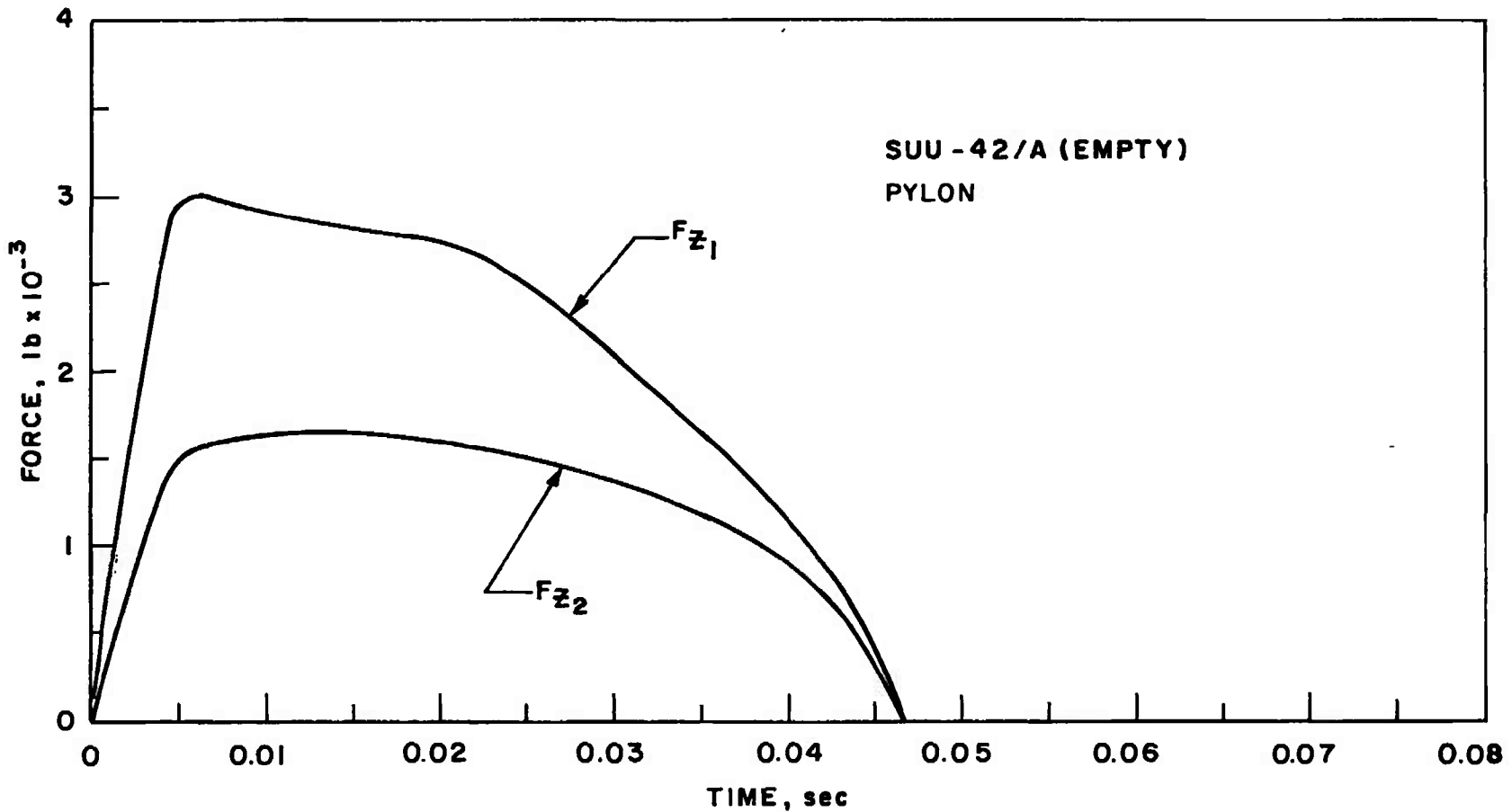


a. Function  $T_1$  for M-117R on MER or TER



b. Function  $T_2$  for BLU-1C/B on MAU-12 Pylon

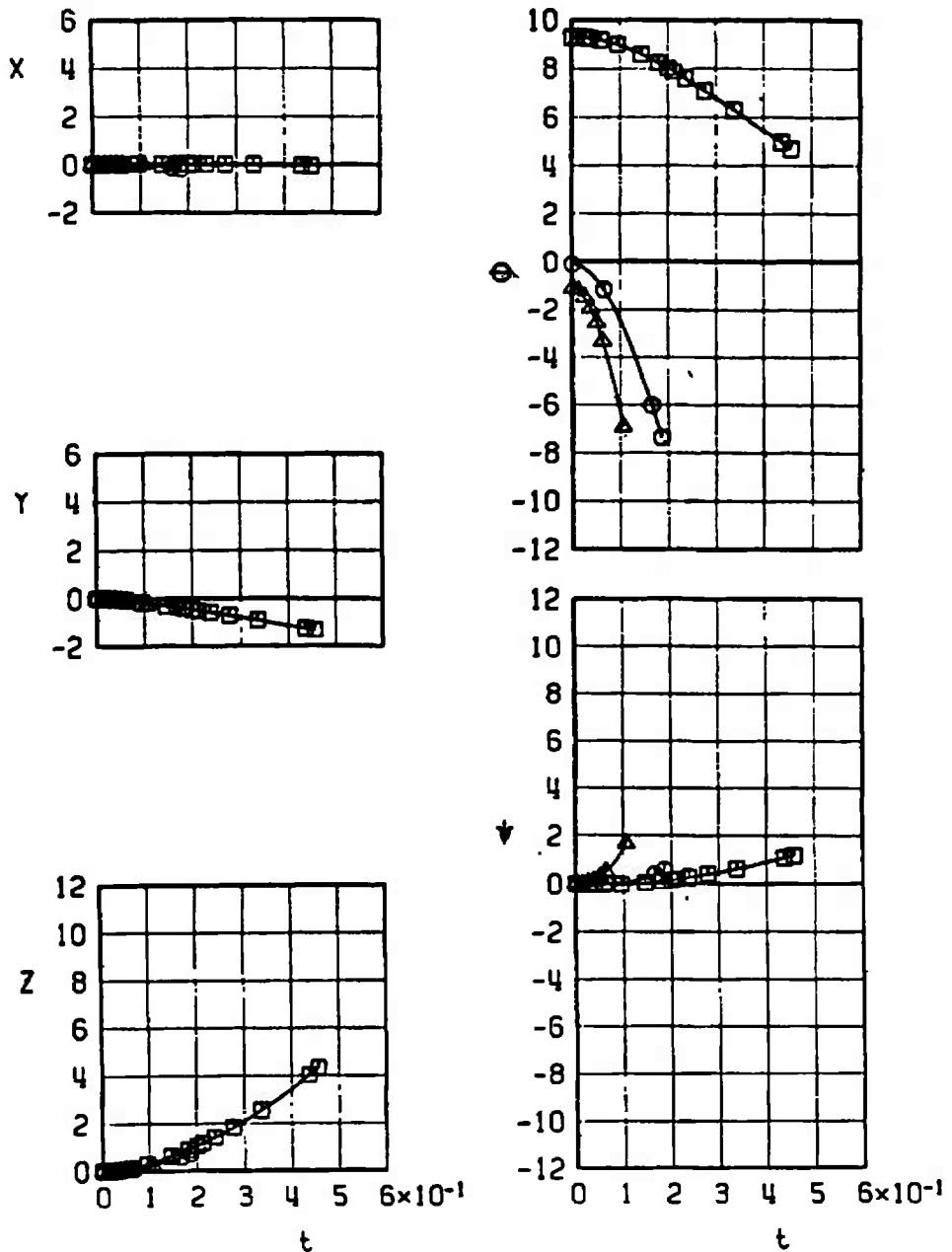
Fig. 13 Ejector Force Functions



c. Function  $T_3$  for Empty SUU-42/A on MAU-12 Pylon  
Fig. 13 Concluded

| SYMBOL | CONF | M <sub>∞</sub> | $\alpha$ | H    | $\ddot{\theta}$ | EJECTOR FORCE |
|--------|------|----------------|----------|------|-----------------|---------------|
| □      | IL   | 0.33           | 12.3     | 4000 | 0               | T I           |
| ○      | IL   | 0.81           | 2.9      | 4000 | 0               | T I           |
| △*     | IL   | 0.95           | 1.9      | 7000 | -70             | T I           |

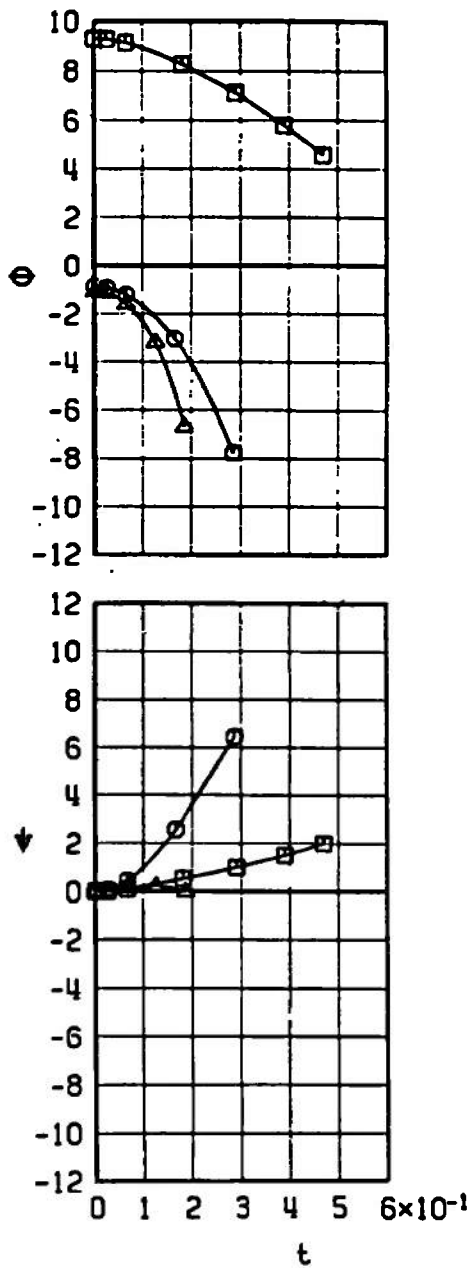
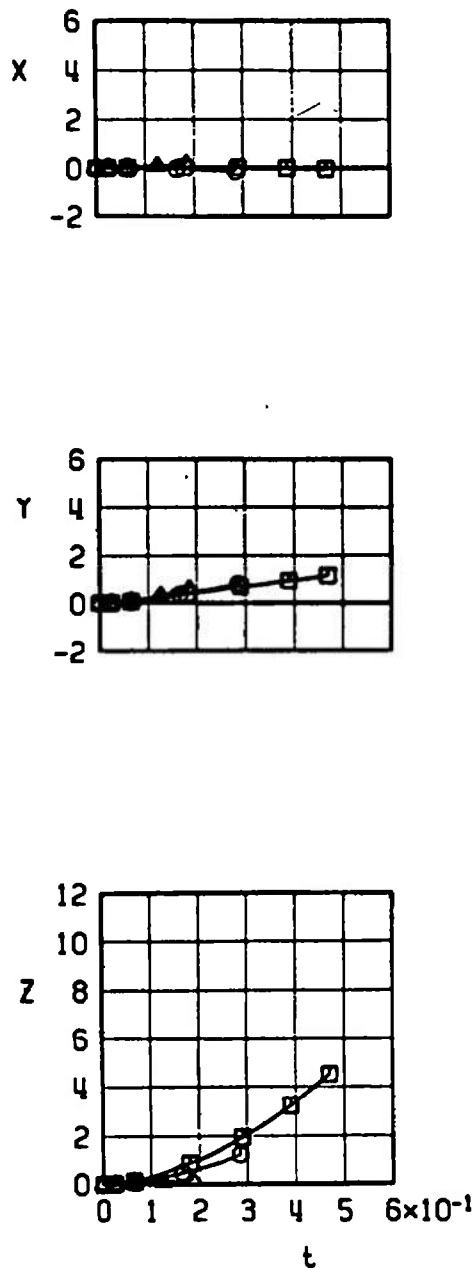
\* STING CONTACT



a. Configuration 1L

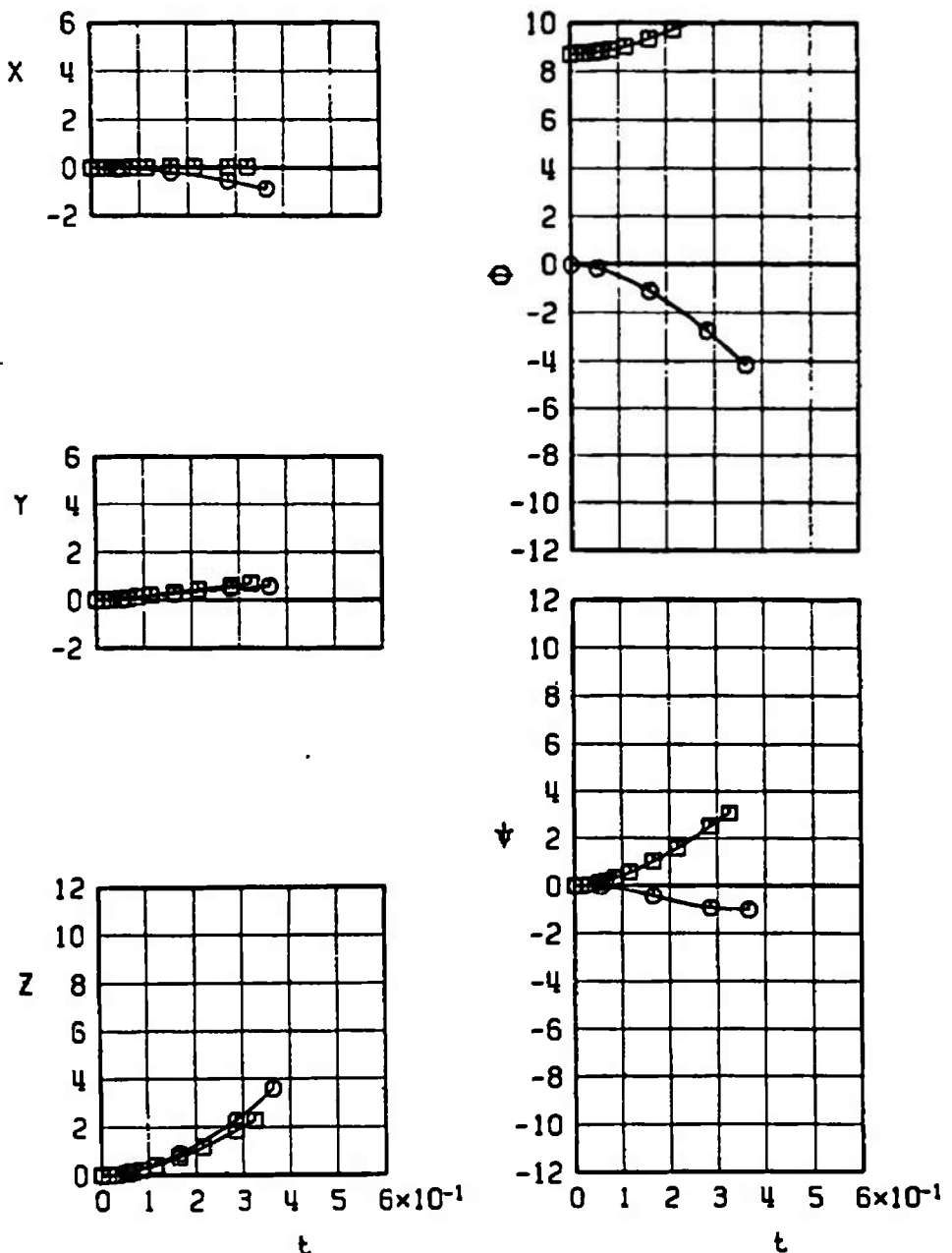
Fig. 14 Effect of Mach Number and Climb Angle on the Separation Trajectories of the M-117R from Center Pylon Station, Inboard and Outboard Pylon Empty

| SYMBOL    | CONF | $M_\infty$ | $\alpha$ | H    | $\bar{e}$ | JECTOR FORCE |
|-----------|------|------------|----------|------|-----------|--------------|
| $\square$ | 2L   | 0.33       | 12.3     | 4000 | 0         | T I          |
| $\circ$   | 2L   | 0.81       | 2.1      | 4000 | 0         | T I          |
| $\Delta$  | 2L   | 0.95       | 1.9      | 7000 | -70       | T I          |



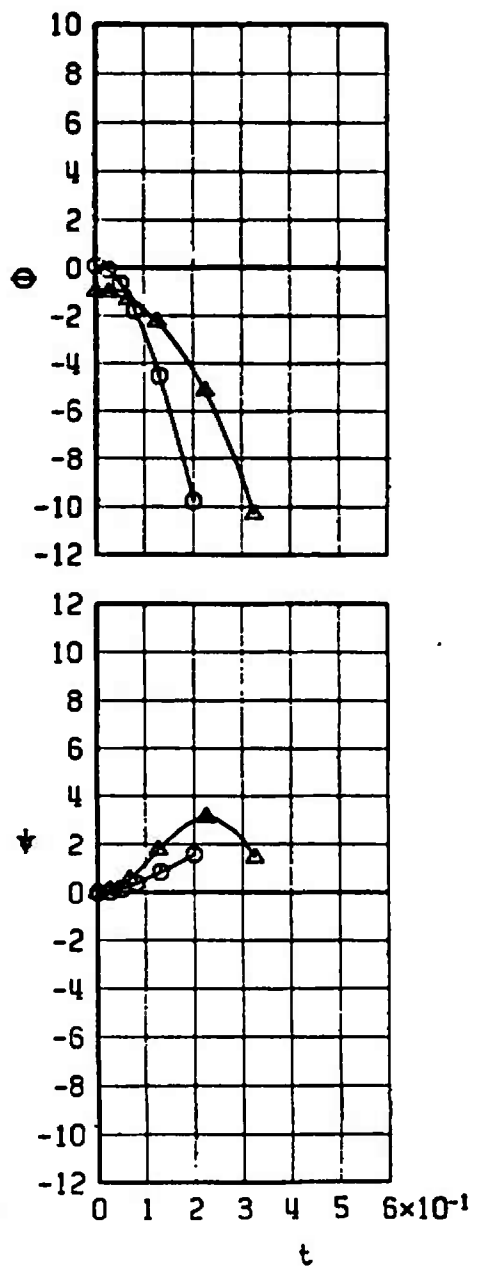
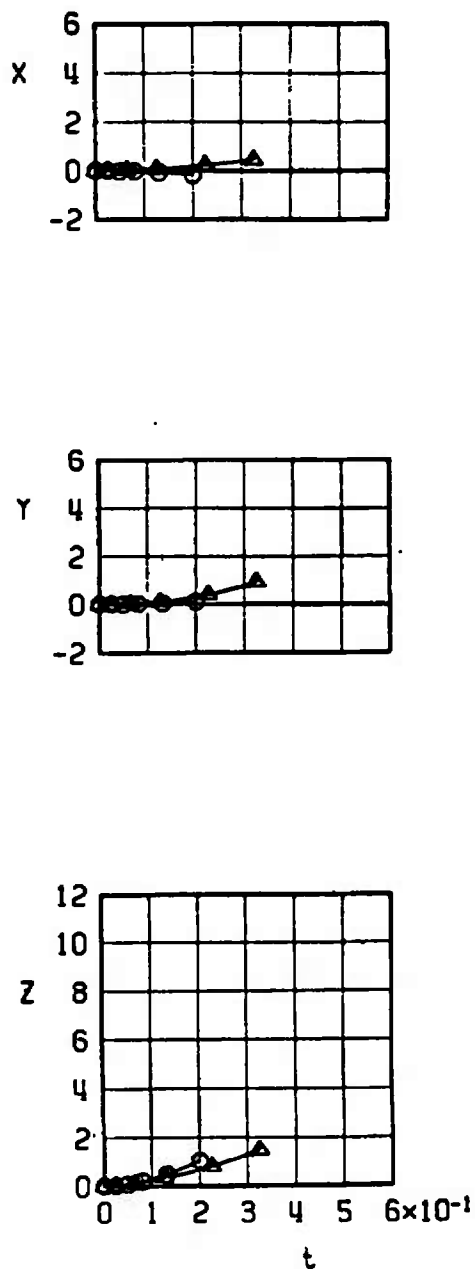
b. Configuration 2L  
Fig. 14 Continued

| SYMBOL    | CONF | $M_\infty$ | $\alpha$ | H    | $\bar{e}$ | EJECTOR FORCE |
|-----------|------|------------|----------|------|-----------|---------------|
| $\square$ | 3L   | 0.33       | 11.7     | 4000 | 0         | T I           |
| $\circ$   | 3L   | 0.81       | 2.9      | 4000 | 0         | T I           |



c. Configuration 3L  
Fig. 14 Continued

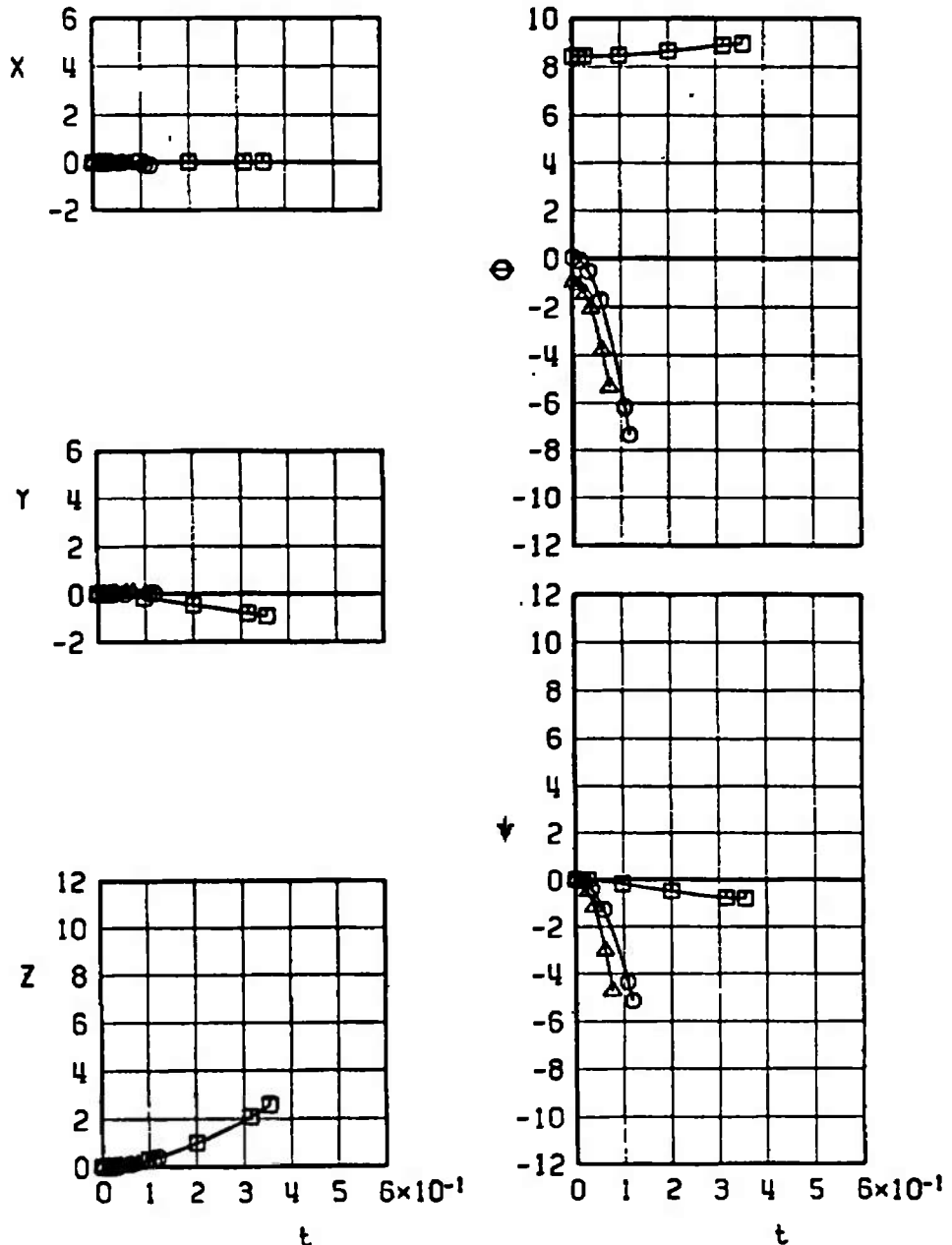
| SYMBOL | CONF | $M_\infty$ | $\alpha$ | H    | $\bar{e}$ | EJECTOR FORCE |
|--------|------|------------|----------|------|-----------|---------------|
| ○      | 4L   | 0.81       | 3.1      | 4000 | 0         | TI            |
| △      | 4L   | 0.95       | 2.0      | 7000 | -70       | TI            |



d. Configuration 4L  
Fig. 14 Continued

| SYMBOL | CONF | $M_\infty$ | $\alpha$ | H    | $\bar{e}$ | EJECTOR FORCE |
|--------|------|------------|----------|------|-----------|---------------|
| □      | 5L   | 0.33       | 11.4     | 4000 | 0         | TI            |
| ○      | 5L   | 0.81       | 2.9      | 4000 | 0         | TI            |
| △*     | 5L   | 0.95       | 1.9      | 7000 | -70       | TI            |

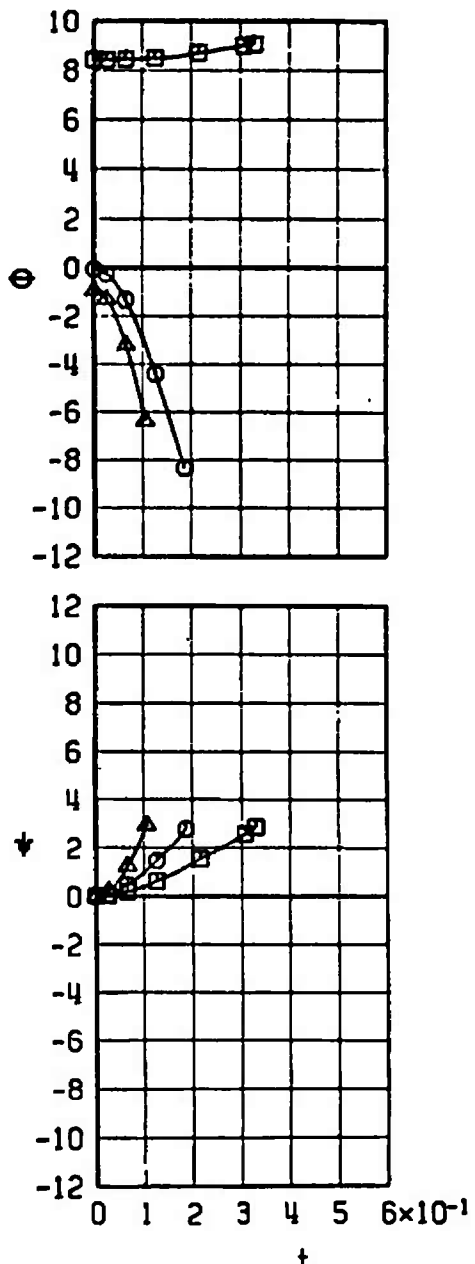
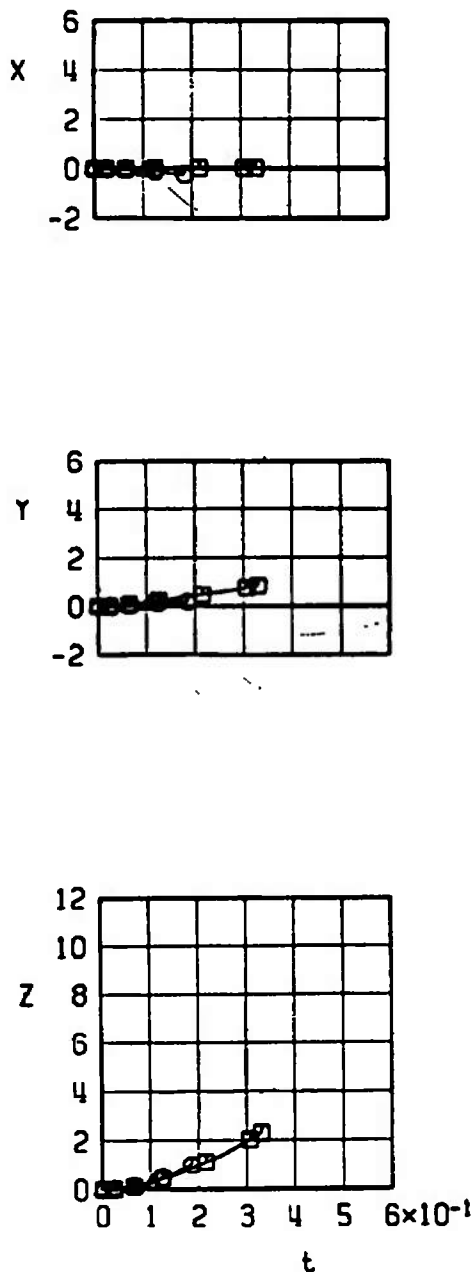
\*STORE CONTACT



e. Configuration 5L  
Fig. 14 Continued

| SYMBOL | CONF | M <sub>0</sub> | $\alpha$ | M    | EJECTOR FORCE |
|--------|------|----------------|----------|------|---------------|
| □      | 6R   | 0.33           | 11.4     | 4000 | 0 T1          |
| ○      | 6R   | 0.81           | 2.9      | 4000 | 0 T1          |
| △*     | 6R   | 0.95           | 1.9      | 7000 | -70 T1        |

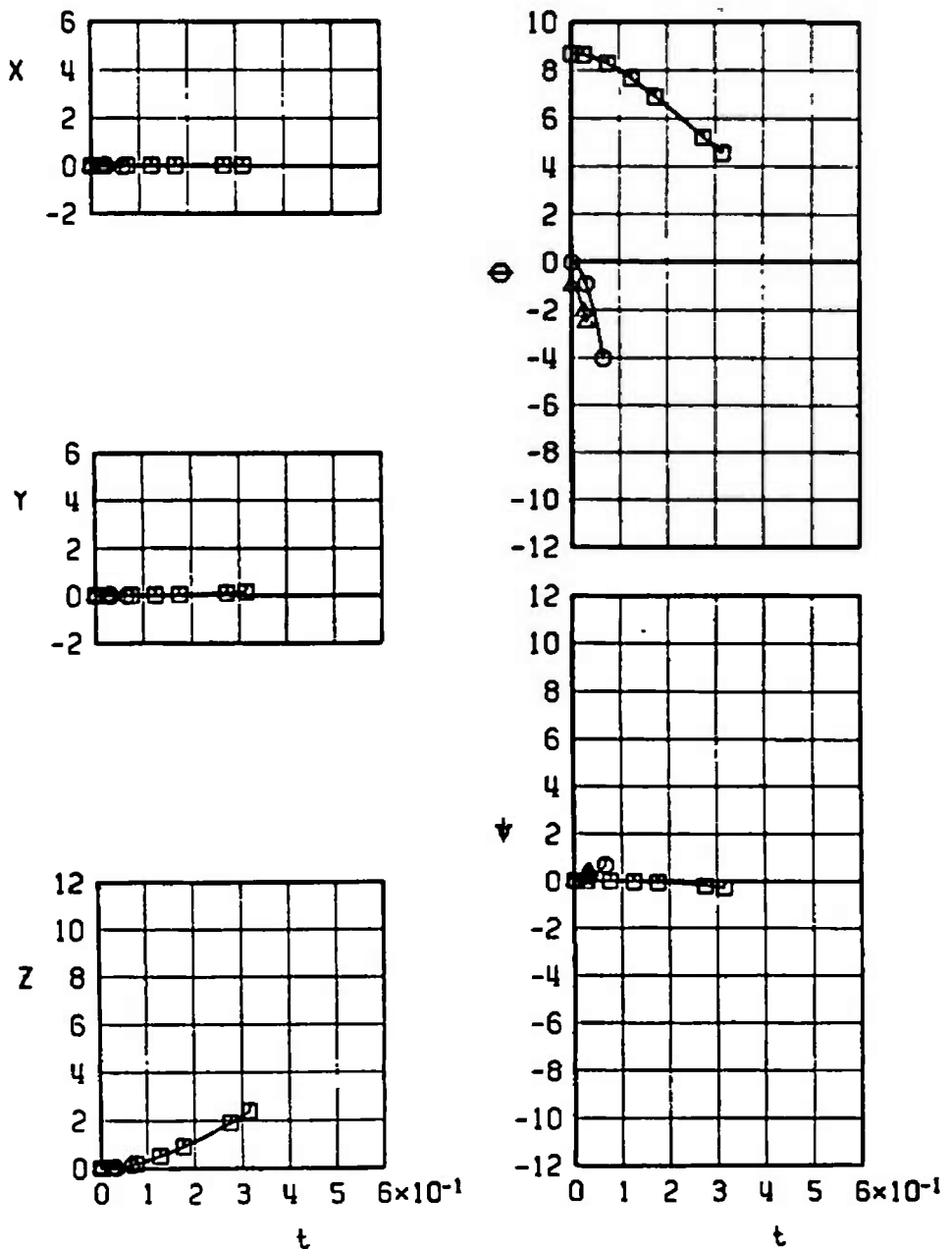
\* STING CONTACT



f. Configuration 6R  
Fig. 14 Continued

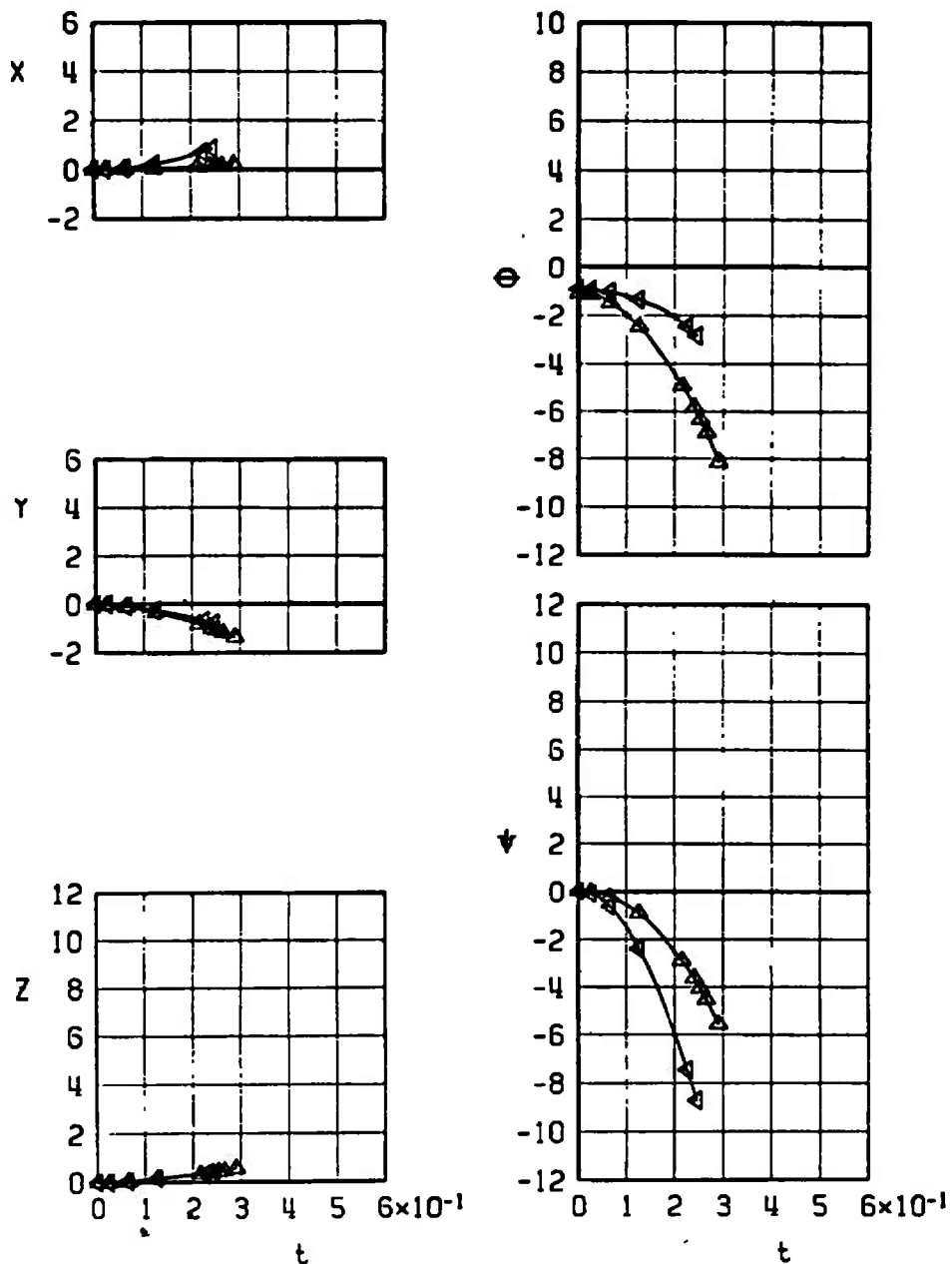
| SYMBOL | CONF | $M_\infty$ | $\alpha$ | H    | EJECTOR FORCE |
|--------|------|------------|----------|------|---------------|
| □      | 7R   | 0.33       | 11.7     | 4000 | 0 TI          |
| ○      | 7R   | 0.81       | 2.9      | 4000 | 0 TI          |
| △*     | 7R   | 0.95       | 1.9      | 7000 | -70 TI        |

\* STORE CONTACT



g. Configuration 7R  
Fig. 14 Concluded

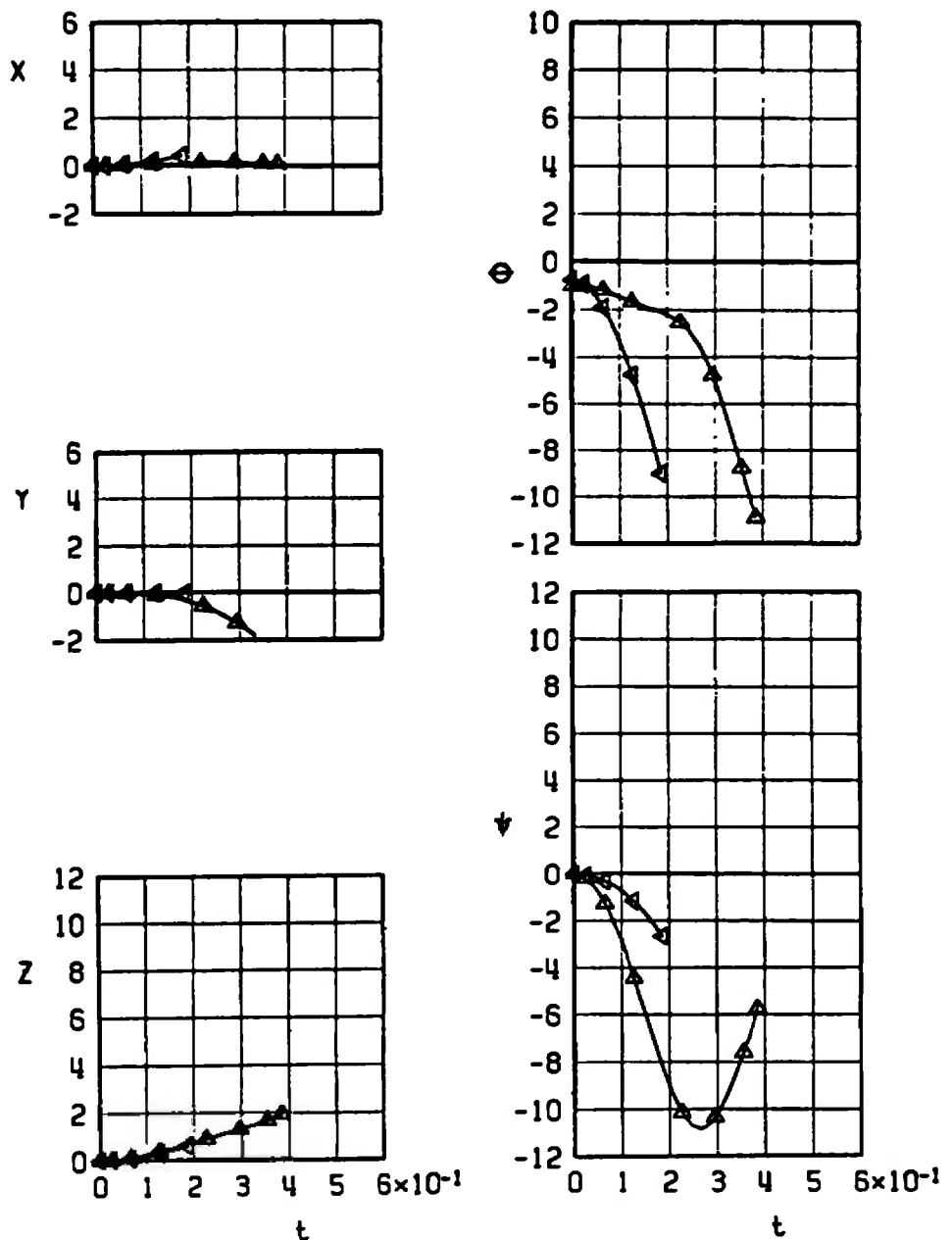
| SYMBOL      | CONF | $M_0$ | $\alpha$ | H    | $\bullet$ | EJECTOR FORCE |
|-------------|------|-------|----------|------|-----------|---------------|
| $\triangle$ | 8R   | 0.78  | 2.1      | 7000 | -70       | T1            |
| $\Delta$    | 8R   | 0.95  | 1.9      | 7000 | -70       | T1            |



a. Configuration 8R

**Fig. 15 Effect of Mach Number and Climb Angle on the Separation Trajectories of the M-117R from Center Pylon Station, Finned BLU-1C/B on Inboard and Outboard Pylon**

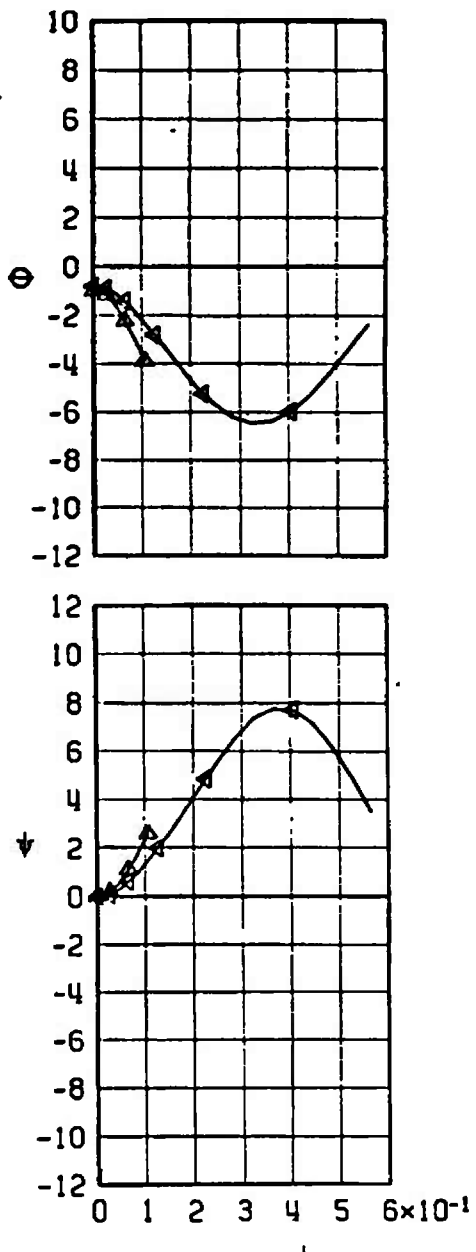
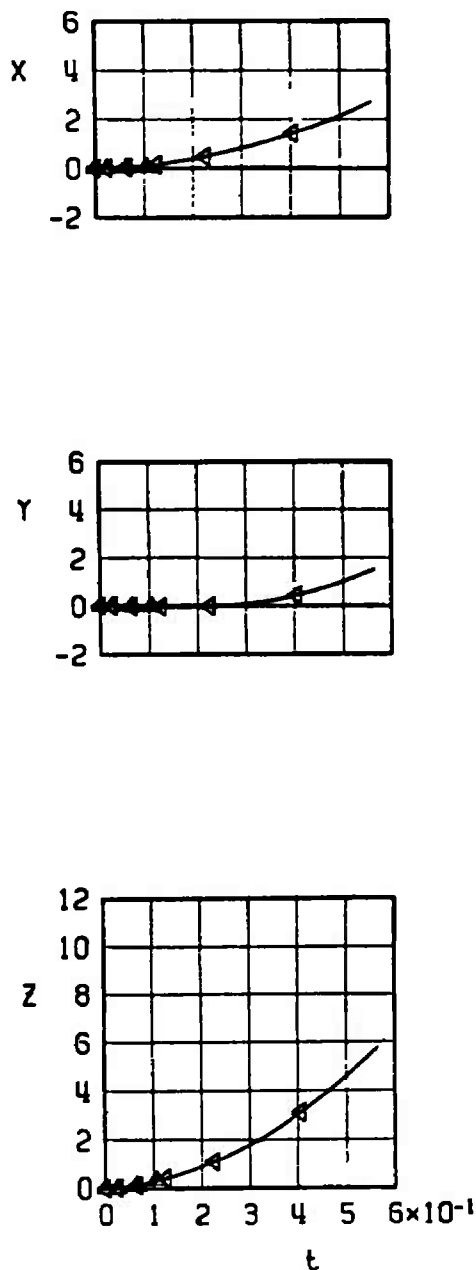
| SYMBOL   | CONF | $M_\infty$ | $\alpha$ | H    | $\bar{e}$ | EJECTOR FORCE |
|----------|------|------------|----------|------|-----------|---------------|
| $\Delta$ | 9R   | 0.78       | 2.2      | 7000 | -70       | T1            |
| $\Delta$ | 9R   | 0.95       | 2.0      | 7000 | -70       | T1            |



b. Configuration 9R  
Fig. 15 Continued

| SYMBOL      | CONF | $M_\infty$ | $\alpha$ | H    | $\bar{H}$ | EJECTOR FORCE |
|-------------|------|------------|----------|------|-----------|---------------|
| $\triangle$ | 10R  | 0.78       | 2.2      | 7000 | -70       | TI            |
| $\Delta^*$  | 10R  | 0.95       | 2.0      | 7000 | -70       | TI            |

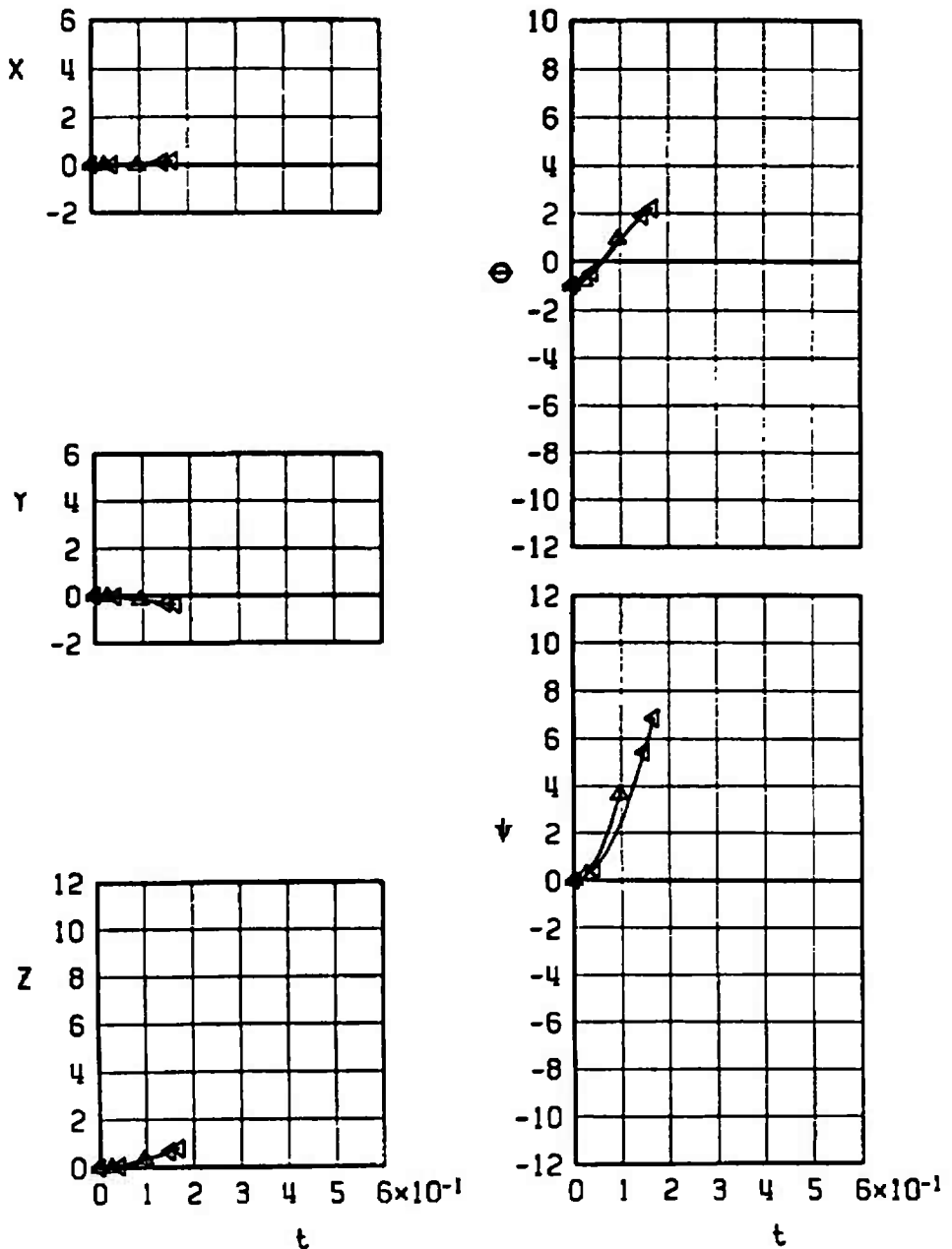
\*STING CONTACT



c. Configuration 10R  
Fig. 15 Continued

| SYMBOL     | CONF | $M_\infty$ | $\alpha$ | H    | $\bar{H}$ | EJECTOR FORCE |
|------------|------|------------|----------|------|-----------|---------------|
| $\Delta^*$ | IIR  | 0.78       | 2.1      | 7000 | -70       | TI            |
| $\Delta^*$ | IIR  | 0.95       | 1.9      | 7000 | -70       | TI            |

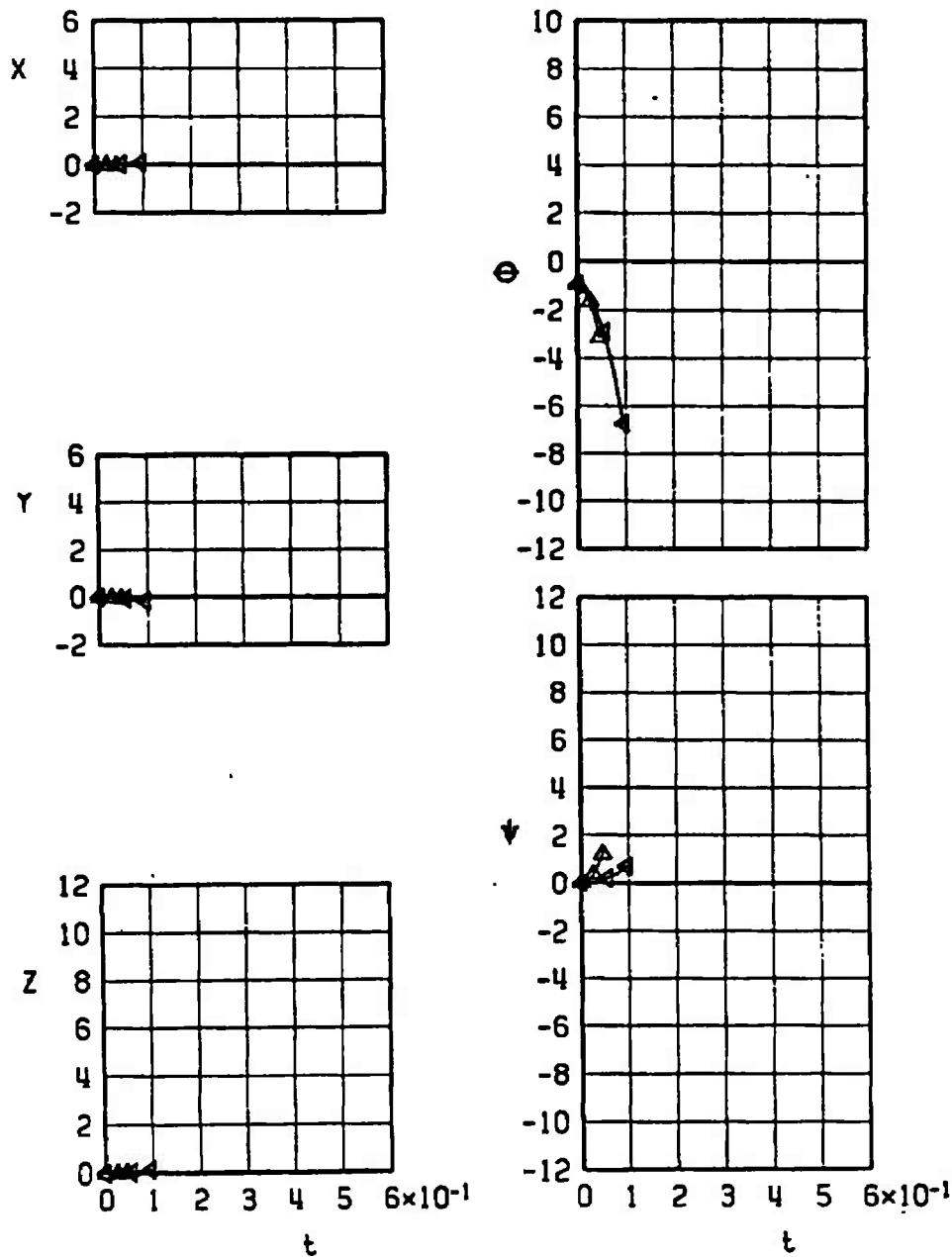
\* STORE CONTACT



d. Configuration 11R  
Fig. 15 Continued

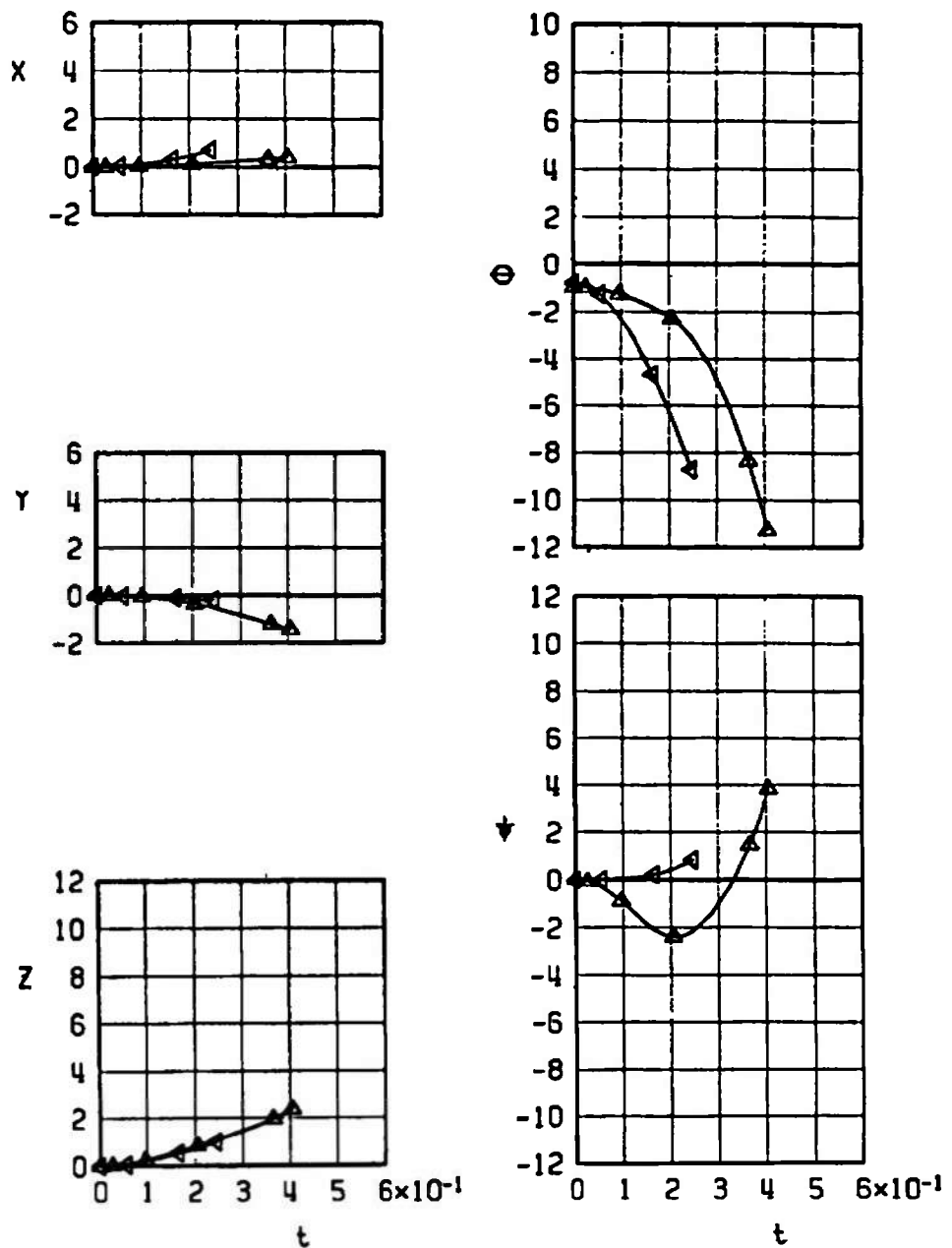
| SYMBOL      | CONF | $M_\infty$ | $\alpha$ | H    | $\bar{H}$ | EJECTOR FORCE |
|-------------|------|------------|----------|------|-----------|---------------|
| $\triangle$ | 12R  | 0.78       | 2.1      | 7000 | -70       | T1            |
| $\Delta^*$  | 12R  | 0.95       | 1.9      | 7000 | -70       | T1            |

\*STORE CONTACT



e. Configuration 12R  
Fig. 15 Concluded

| SYMBOL | CONF | $M_\infty$ | $\alpha$ | H    | $\bar{\epsilon}$ | EJECTOR FORCE |
|--------|------|------------|----------|------|------------------|---------------|
| ▲      | 13R  | 0.78       | 2.2      | 7000 | -70              | T1            |
| △      | 13R  | 0.95       | 1.9      | 7000 | -70              | T1            |

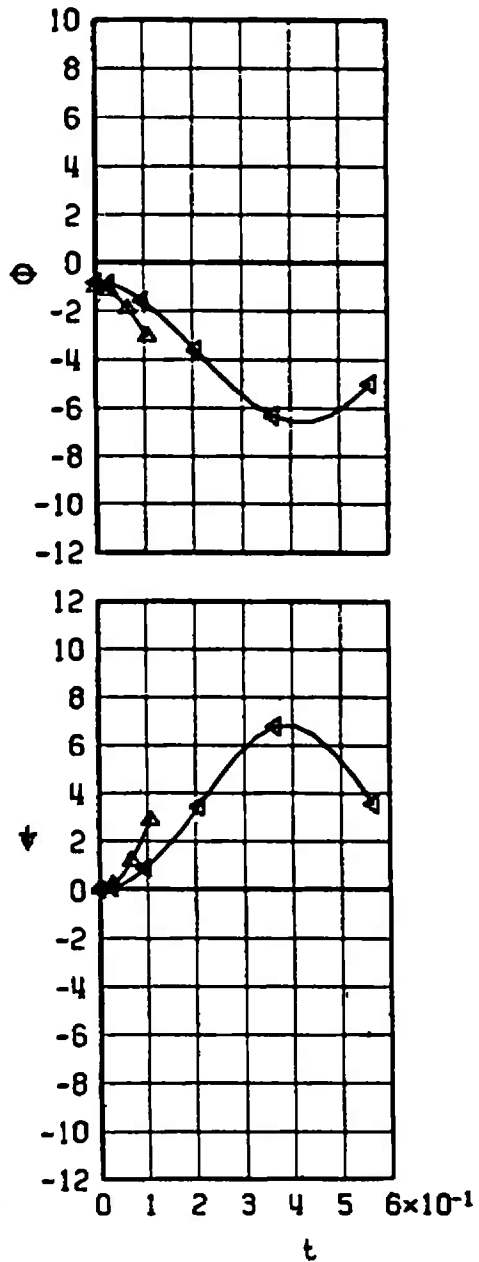
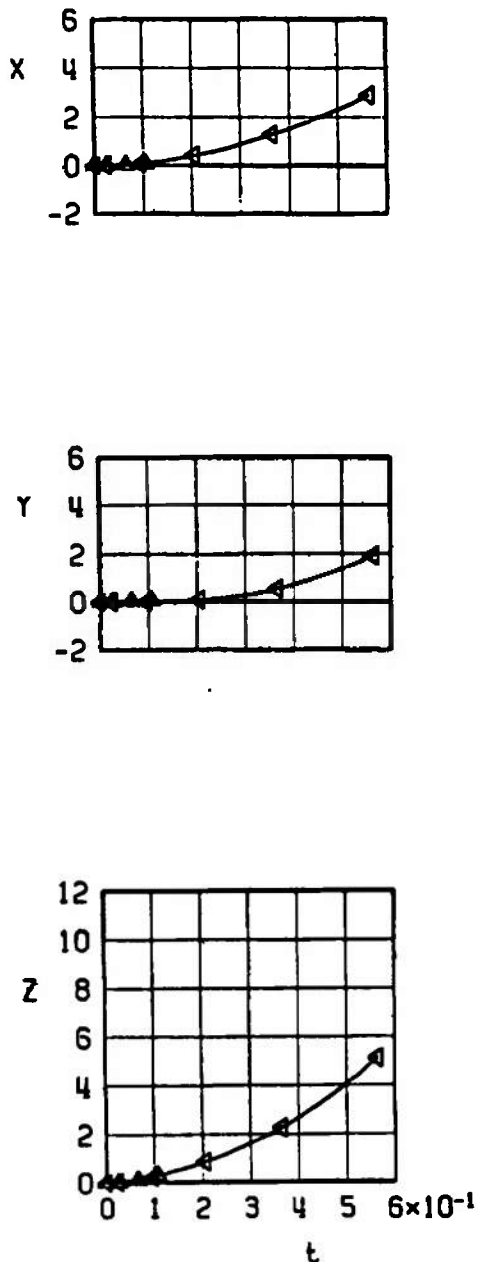


a. Configuration 13R

Fig. 16 Effect of Mach Number on the Separation Trajectories of M-117R from Center Pylon Station, Outboard Pylon Empty, and M-117R on Inboard Pylon

| SYMBOL | CONF | M <sub>∞</sub> | $\alpha$ | H    | • EJECTOR FORCE |    |
|--------|------|----------------|----------|------|-----------------|----|
| △      | I4R  | 0.78           | 2.1      | 7000 | -70             | T1 |
| △*     | I4R  | 0.95           | 1.9      | 7000 | -70             | T1 |

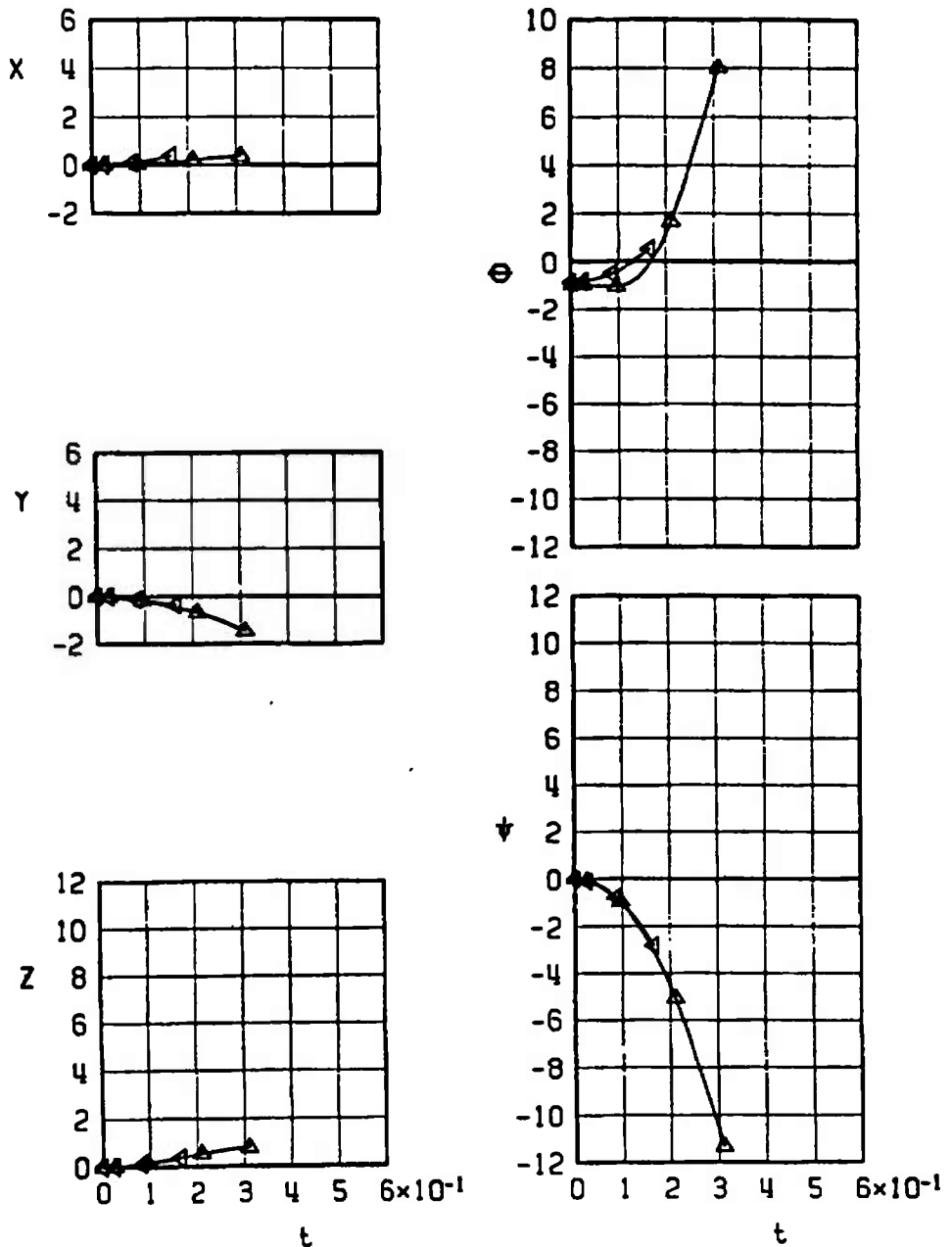
\* STORE CONTACT



b. Configuration 14R  
Fig. 16 Continued

| SYMBOL     | CONF | $M_\infty$ | $\alpha$ | H    | $\bar{e}$ | EJECTOR FORCE |
|------------|------|------------|----------|------|-----------|---------------|
| $\Delta^*$ | 15R  | 0.78       | 2.1      | 7000 | -70       | T I           |
| $\Delta$   | 15R  | 0.95       | 1.9      | 7000 | -70       | T I           |

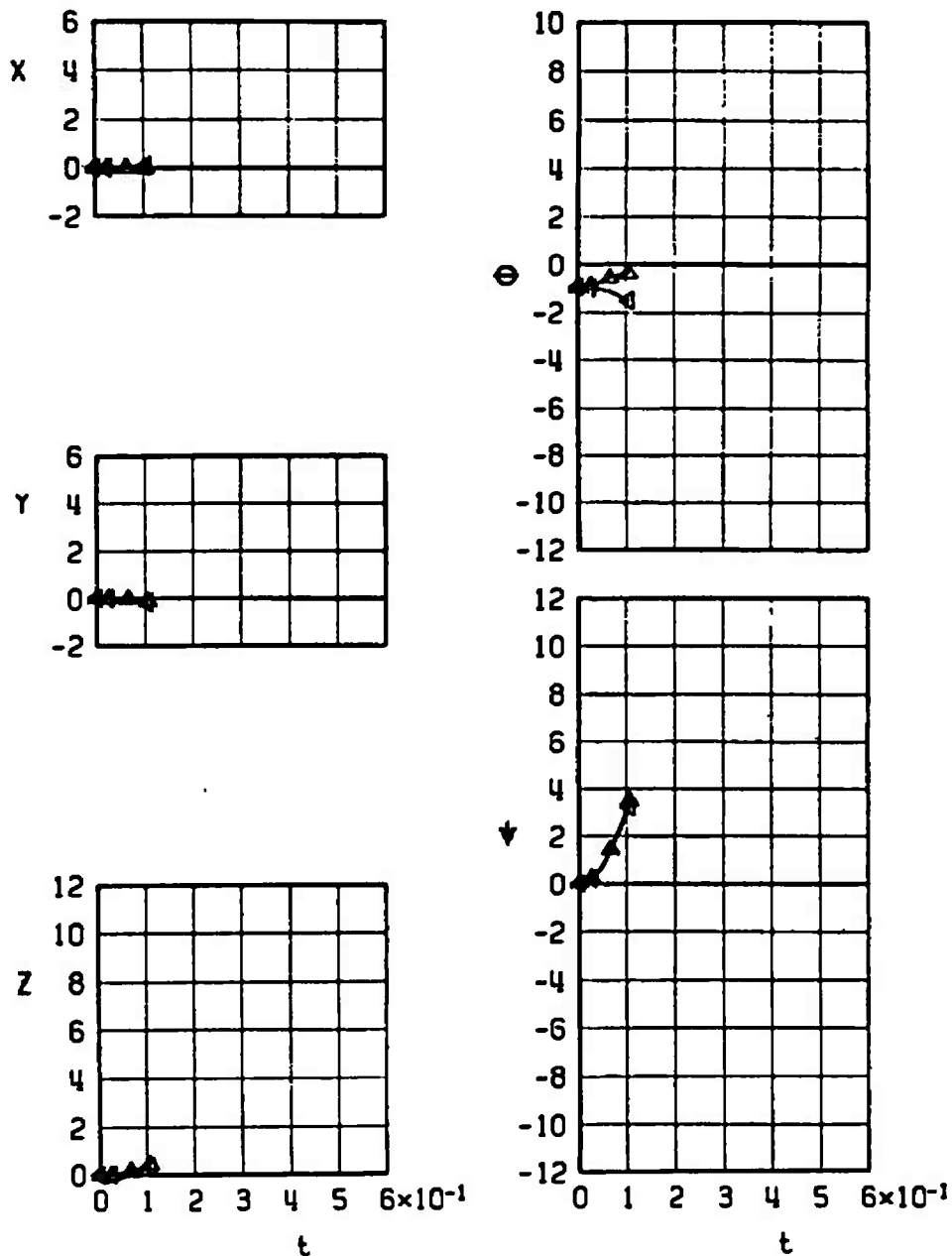
\*STING CONTACT



c. Configuration 15R  
Fig. 16 Continued

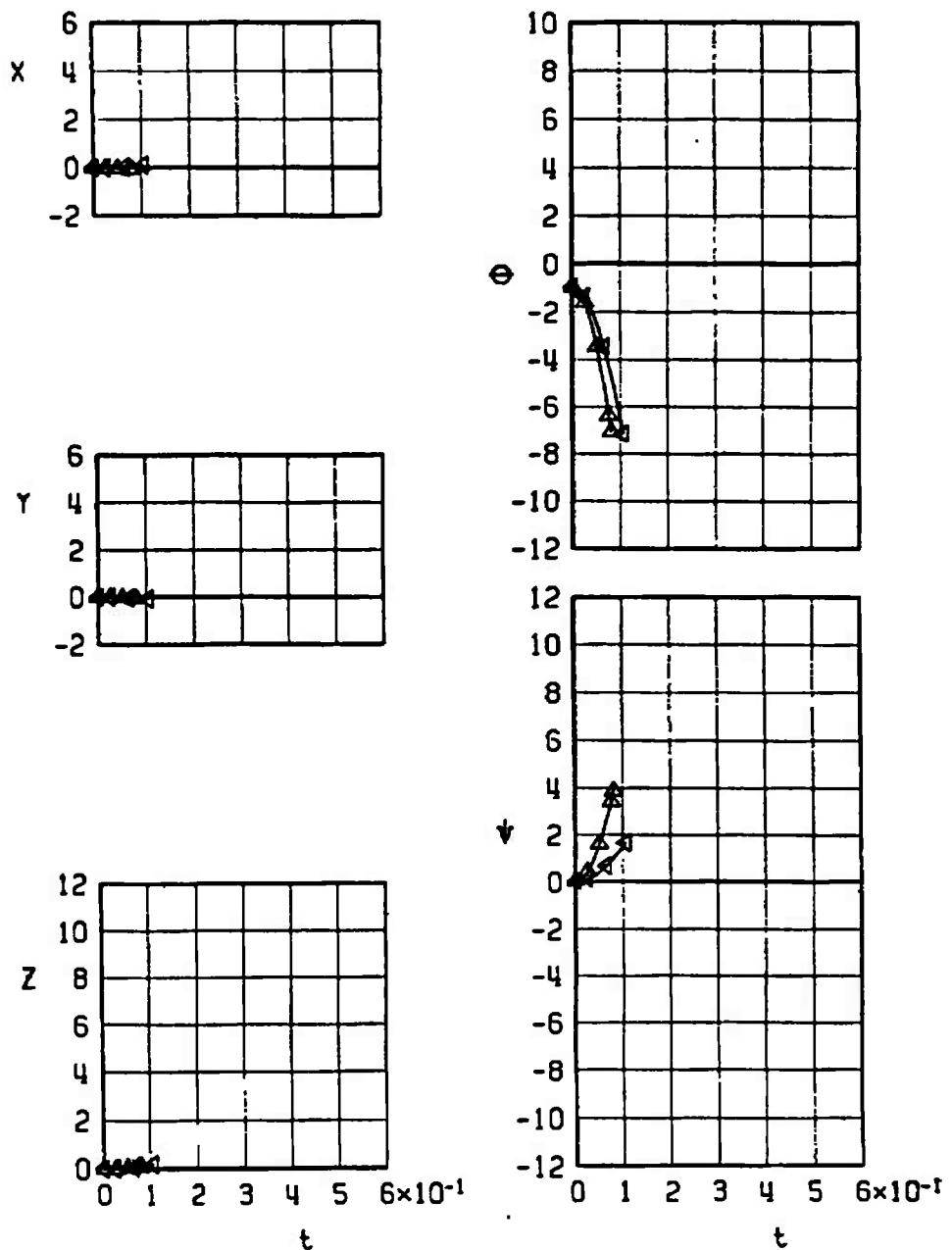
| SYMBOL        | CONF | $M_\infty$ | $\alpha$ | H    | $\bar{e}$ | EJECTOR FORCE |
|---------------|------|------------|----------|------|-----------|---------------|
| $\triangle^*$ | 16R  | 0.78       | 2.1      | 7000 | -70       | T1            |
| $\Delta^*$    | 16R  | 0.95       | 1.9      | 7000 | -70       | T1            |

\*STING CONTACT



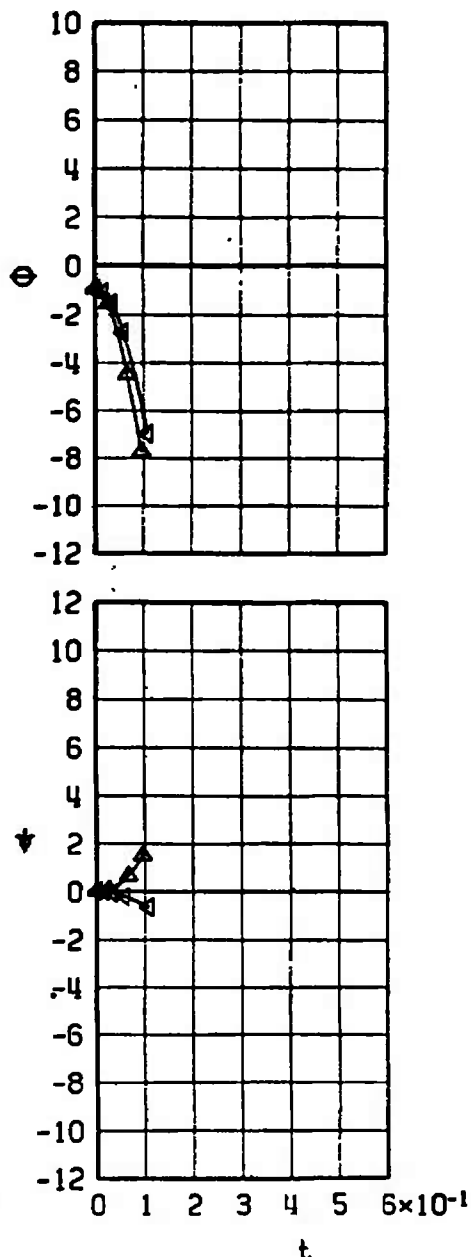
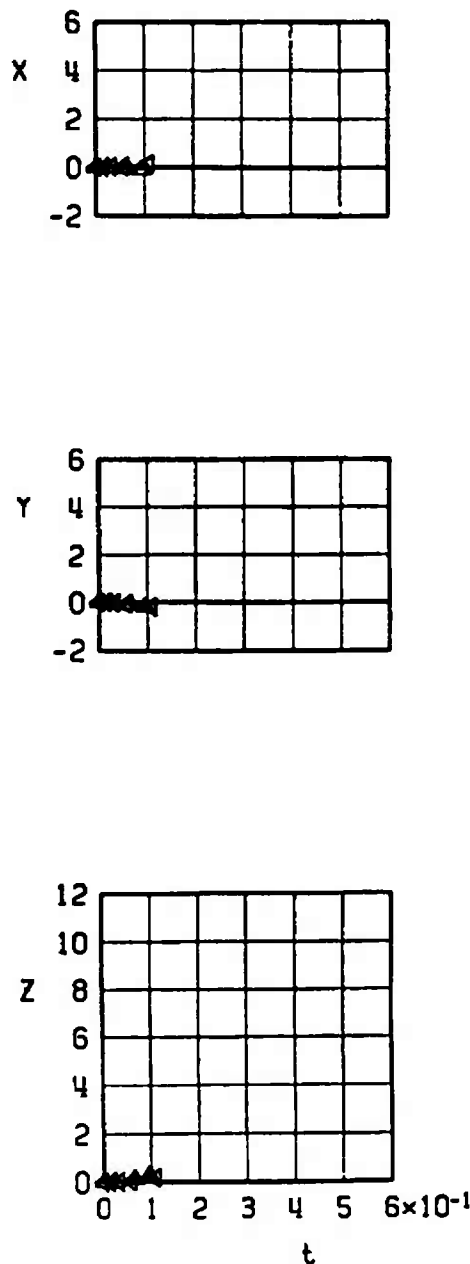
d. Configuration 16R  
Fig. 16 Continued

| SYMBOL      | CONF | $M_\infty$ | $\alpha$ | H    | $\bar{e}$ | EJECTOR FORCE |
|-------------|------|------------|----------|------|-----------|---------------|
| $\triangle$ | 17R  | 0.78       | 2.1      | 7000 | -70       | TI            |
| $\Delta$    | 17R  | 0.95       | 1.9      | 7000 | -70       | TI            |



e. Configuration 17R  
Fig. 16 Continued

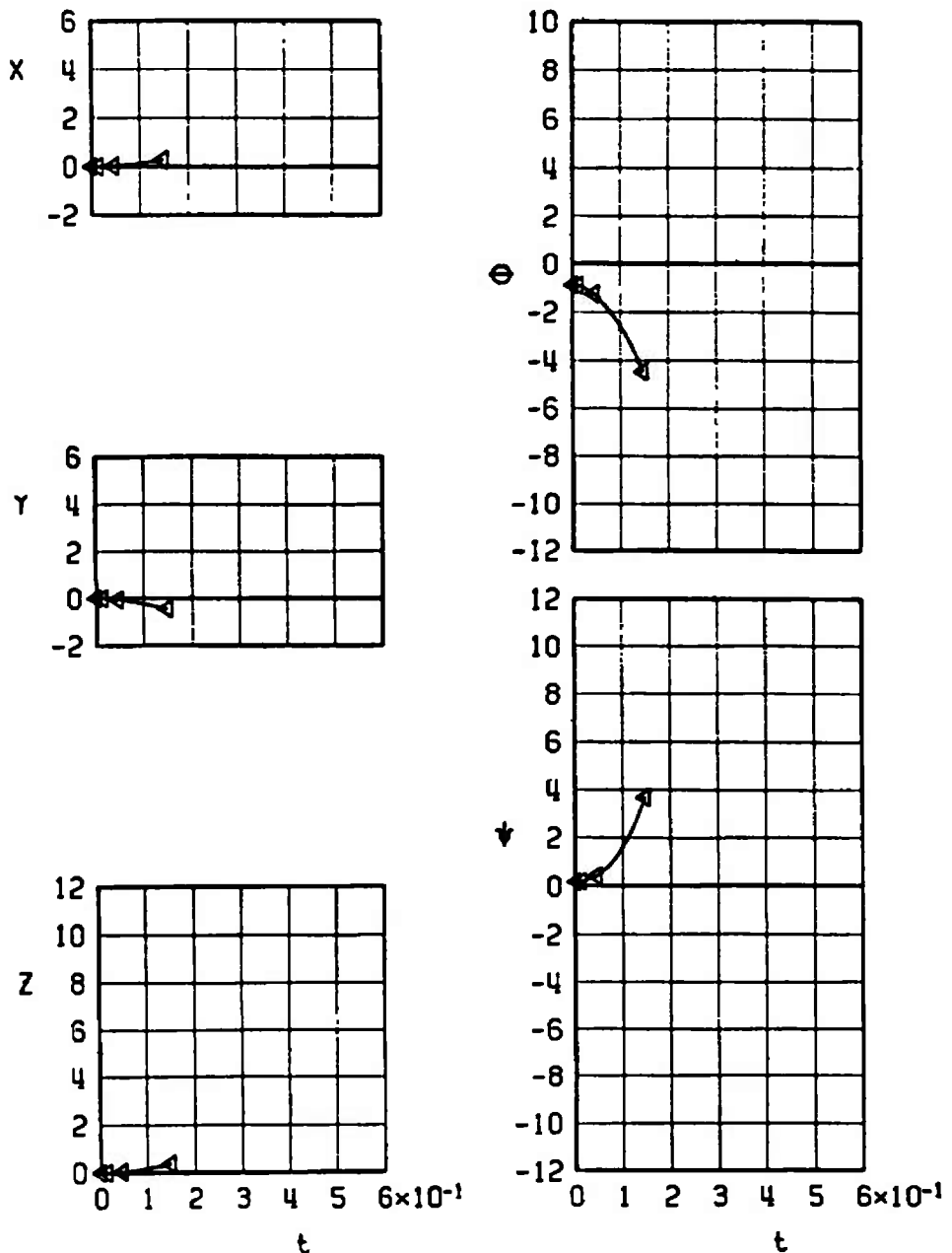
| SYMBOL      | CONF | $M_\infty$ | $\alpha$ | H    | $\bar{H}$ | EJECTOR FORCE |
|-------------|------|------------|----------|------|-----------|---------------|
| $\triangle$ | 18R  | 0.78       | 2.1      | 7000 | -70       | T1            |
| $\triangle$ | 18R  | 0.95       | 1.9      | 7000 | -70       | T1            |



f. Configuration 18R  
Fig. 16 Concluded

| SYMBOL        | CONF | M <sub>∞</sub> | $\alpha$ | H    | $\bar{e}$ | EJECTOR FORCE |
|---------------|------|----------------|----------|------|-----------|---------------|
| $\triangle^*$ | 19L  | 0.78           | 2.1      | 7000 | -70       | T1            |
| $\Delta^*$    | 19L  | 0.95           | 1.9      | 7000 | -70       | T1            |

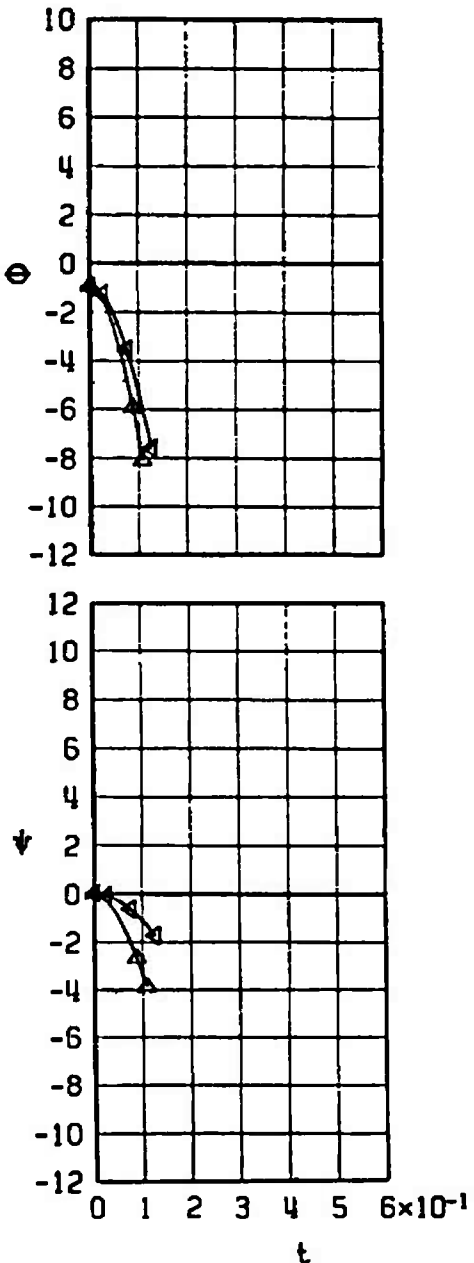
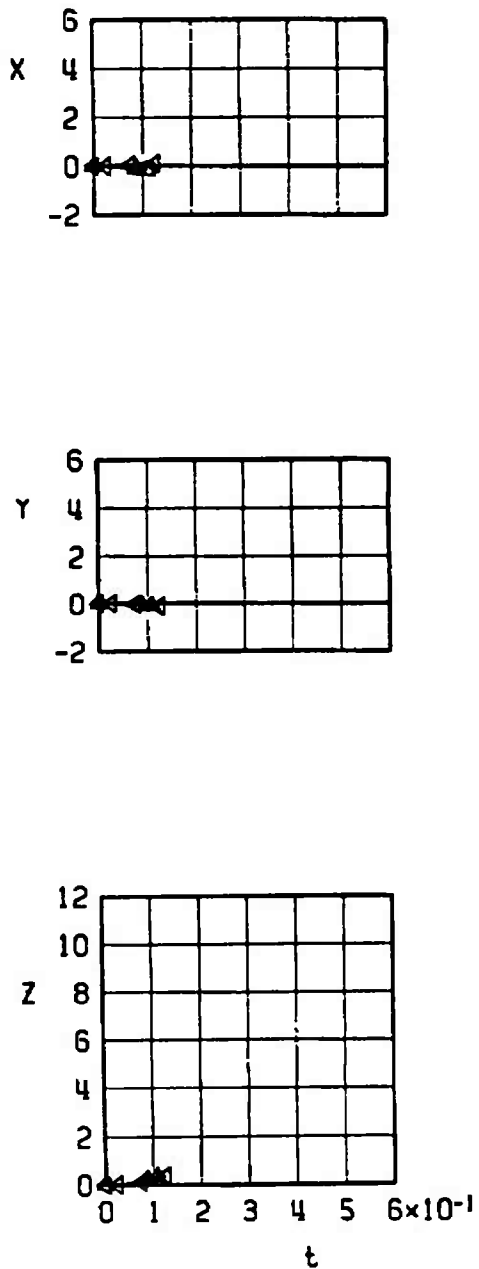
\*STING CONTACT



a. Configuration 19L

Fig. 17 Effect of Mach Number on the Separation Trajectories of the M-117R from Center Pylon Station, Unfinned BLU-1C/B on Outboard and Inboard Pylons

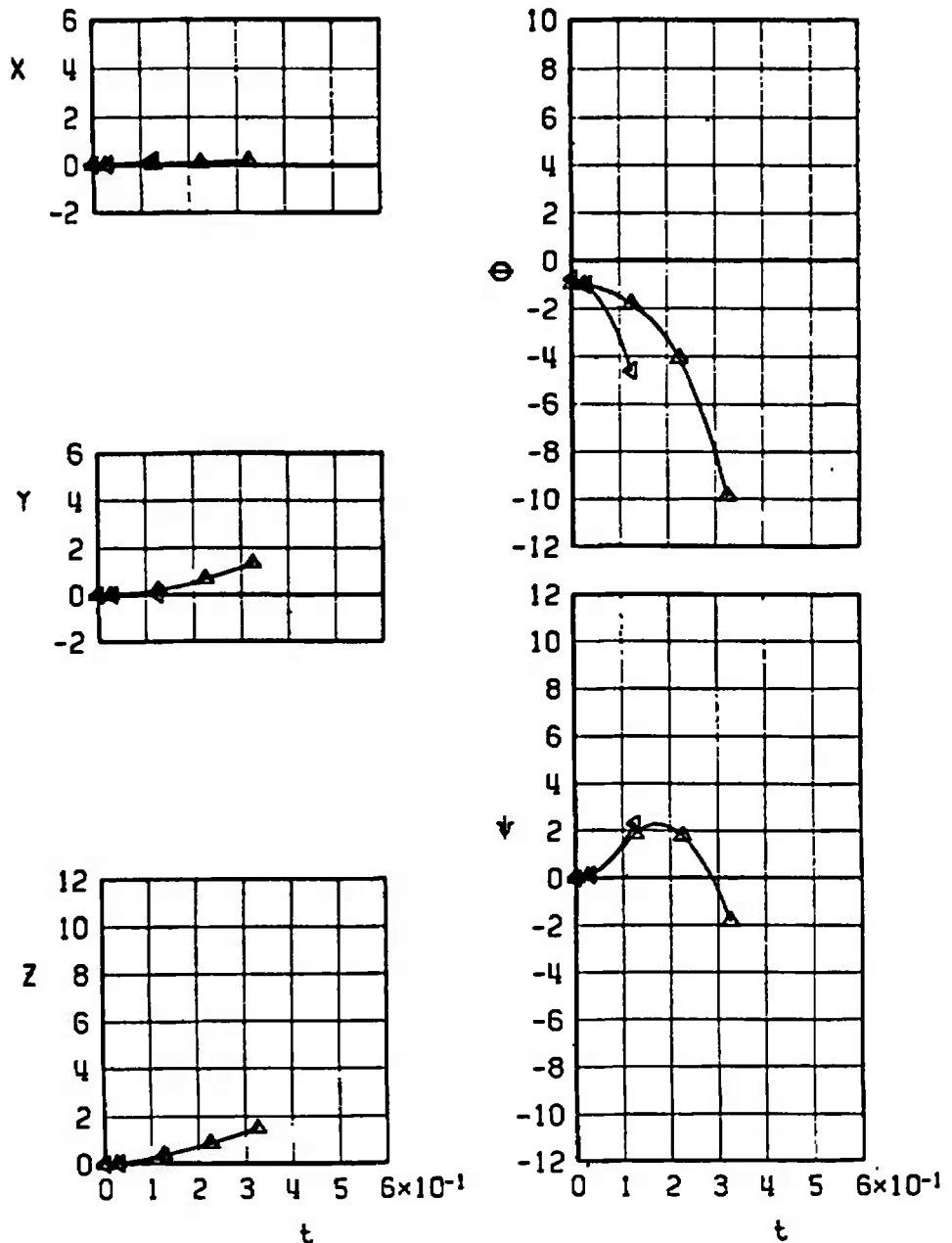
| SYMBOL      | CONF | $M_\infty$ | $\alpha$ | H    | $\bar{e}$ | EJECTOR FORCE |
|-------------|------|------------|----------|------|-----------|---------------|
| $\triangle$ | 20L  | 0.78       | 2.1      | 7000 | -70       | T1            |
| $\Delta$    | 20L  | 0.95       | 1.9      | 7000 | -70       | T1            |



b. Configuration 20L  
Fig. 17 Concluded

| SYMBOL     | CONF | $M_\infty$ | $\alpha$ | H    | $\bar{\epsilon}$ | EJECTOR FORCE |
|------------|------|------------|----------|------|------------------|---------------|
| $\Delta^*$ | 2IL  | 0.78       | 2.2      | 7000 | -70              | T1            |
| $\Delta$   | 2IL  | 0.95       | 1.9      | 7000 | -70              | T1            |

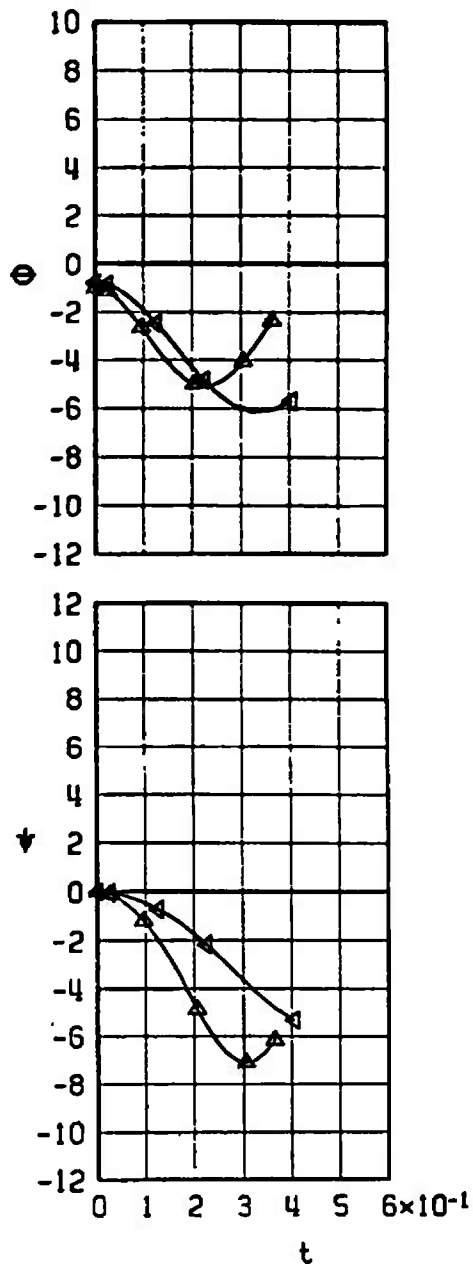
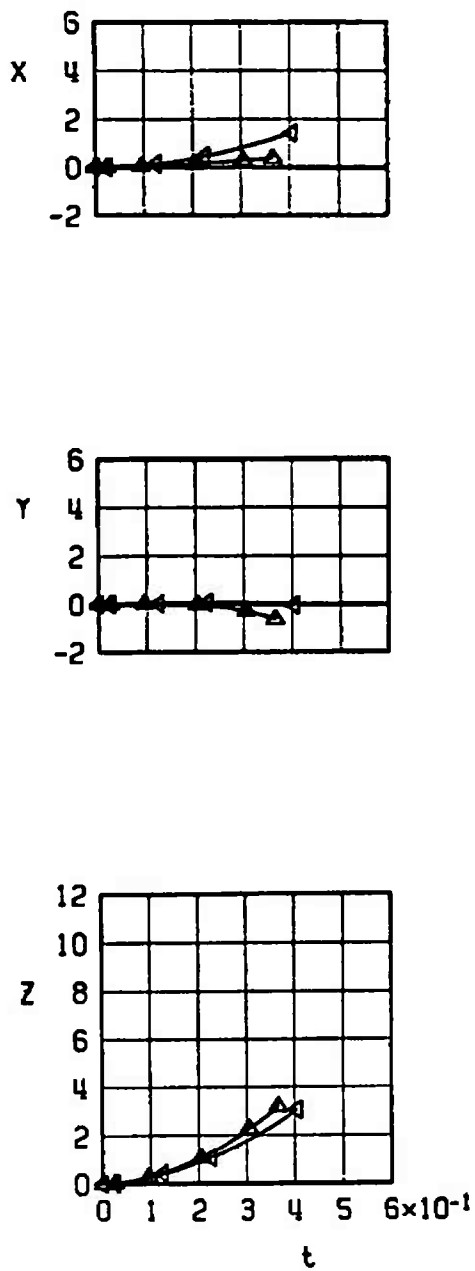
\*STORE CONTACT



a. Configuration 21L

Fig. 18 Effect of Mach Number on the Separation Trajectories of the M-117R from Center Pylon Station, M-117R on Inboard, and SUU-42/A on Outboard Pylon

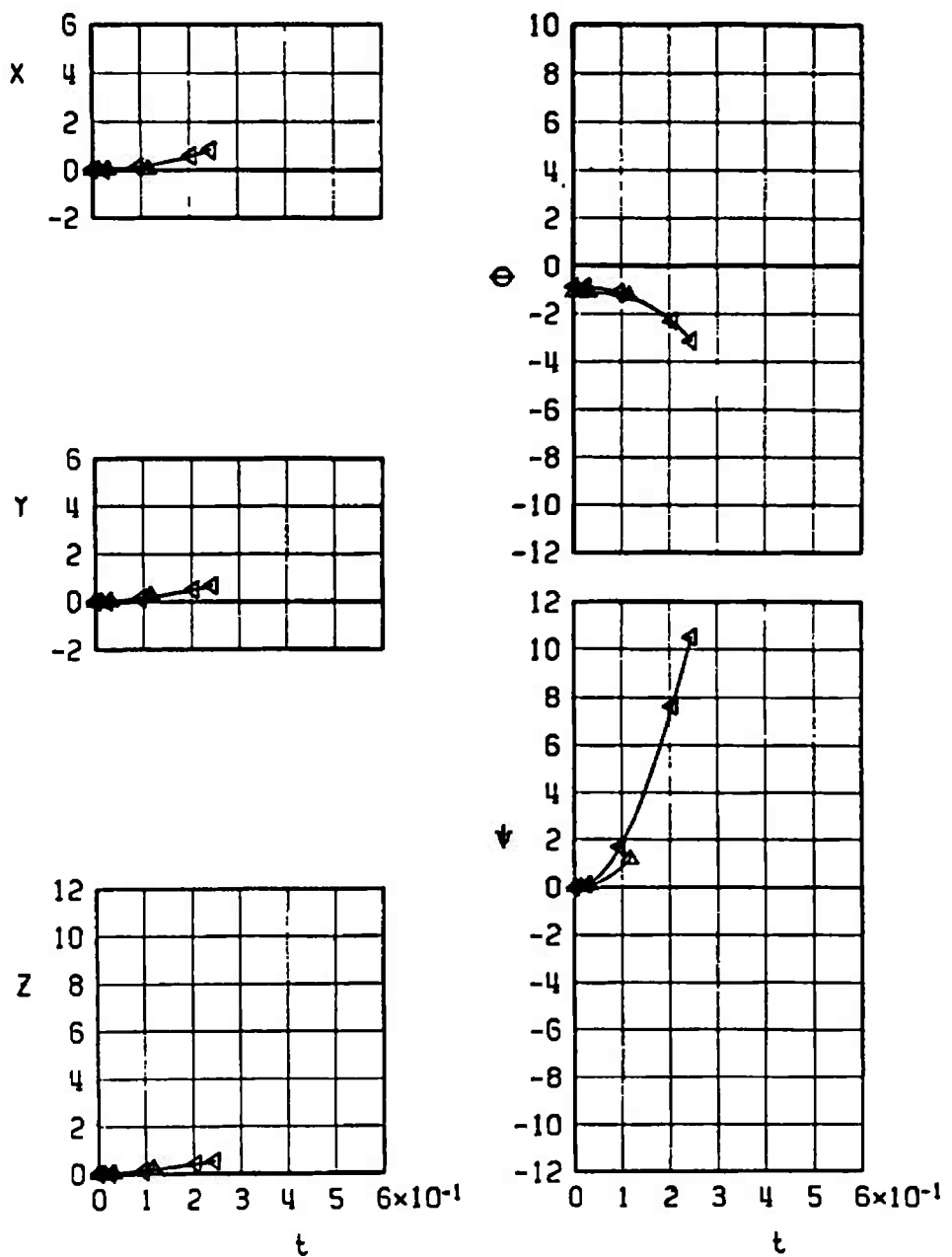
| SYMBOL               | CONF | $M_\infty$ | $\alpha$ | H    | $\bar{c}$ | EJECTOR FORCE |
|----------------------|------|------------|----------|------|-----------|---------------|
| $\blacktriangleleft$ | 22L  | 0.78       | 2.1      | 7000 | -70       | T1            |
| $\triangle$          | 22L  | 0.95       | 1.9      | 7000 | -70       | T1            |



b. Configuration 22L  
Fig. 18 Continued

| SYMBOL        | CONF | $M_\infty$ | $\alpha$ | H    | $\bar{e}$ | EJECTOR FORCE |
|---------------|------|------------|----------|------|-----------|---------------|
| $\triangle$   | 23L  | 0.78       | 2.1      | 7000 | -70       | T1            |
| $\triangle^*$ | 23L  | 0.95       | 1.9      | 7000 | -70       | T1            |

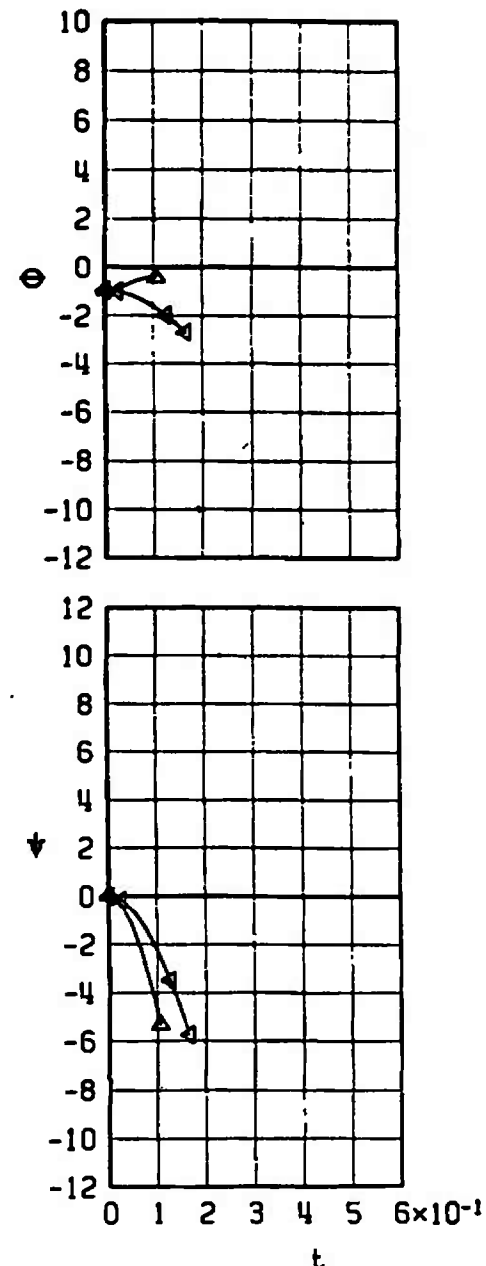
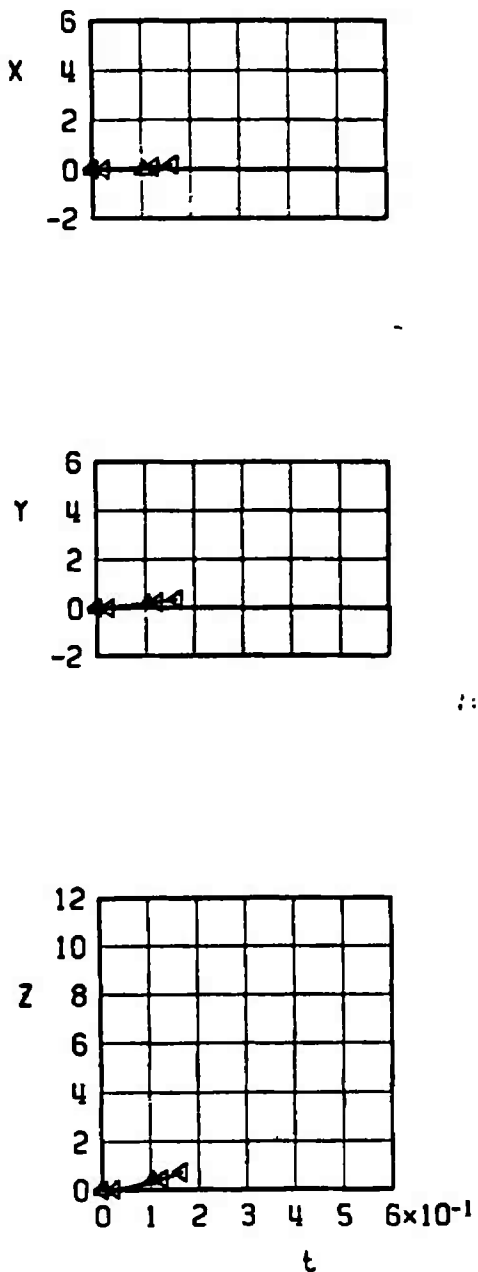
\* STING CONTACT



c. Configuration 23L  
Fig. 18 Continued

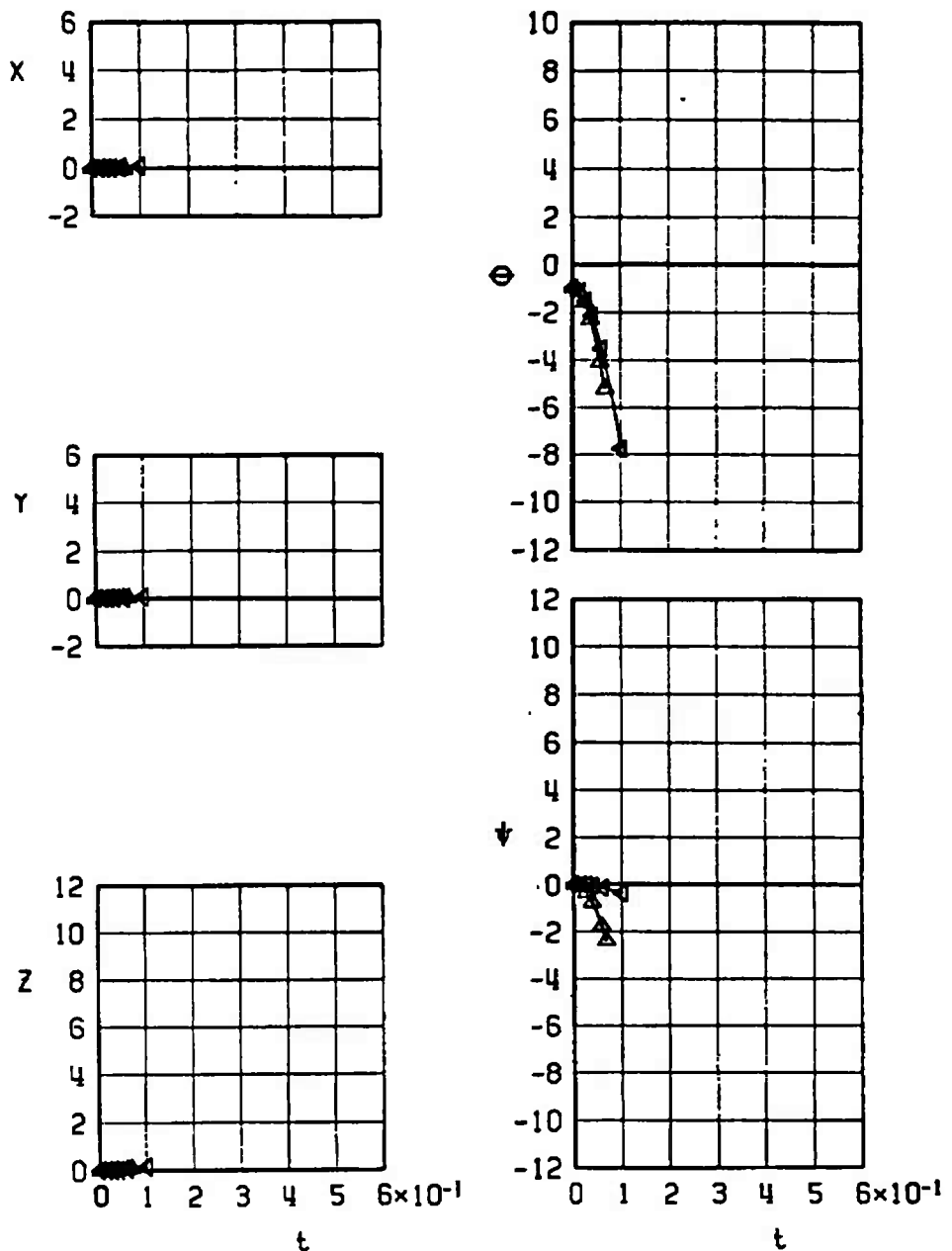
| SYMBOL        | CONF | M <sub>a</sub> | $\alpha$ | H    | $\bar{H}$ | EJECTOR FORCE  |
|---------------|------|----------------|----------|------|-----------|----------------|
| $\triangle^*$ | 24L  | 0.78           | 2.1      | 7000 | -70       | T <sub>1</sub> |
| $\triangle^*$ | 24L  | 0.95           | 1.9      | 7000 | -70       | T <sub>1</sub> |

\*STING CONTACT



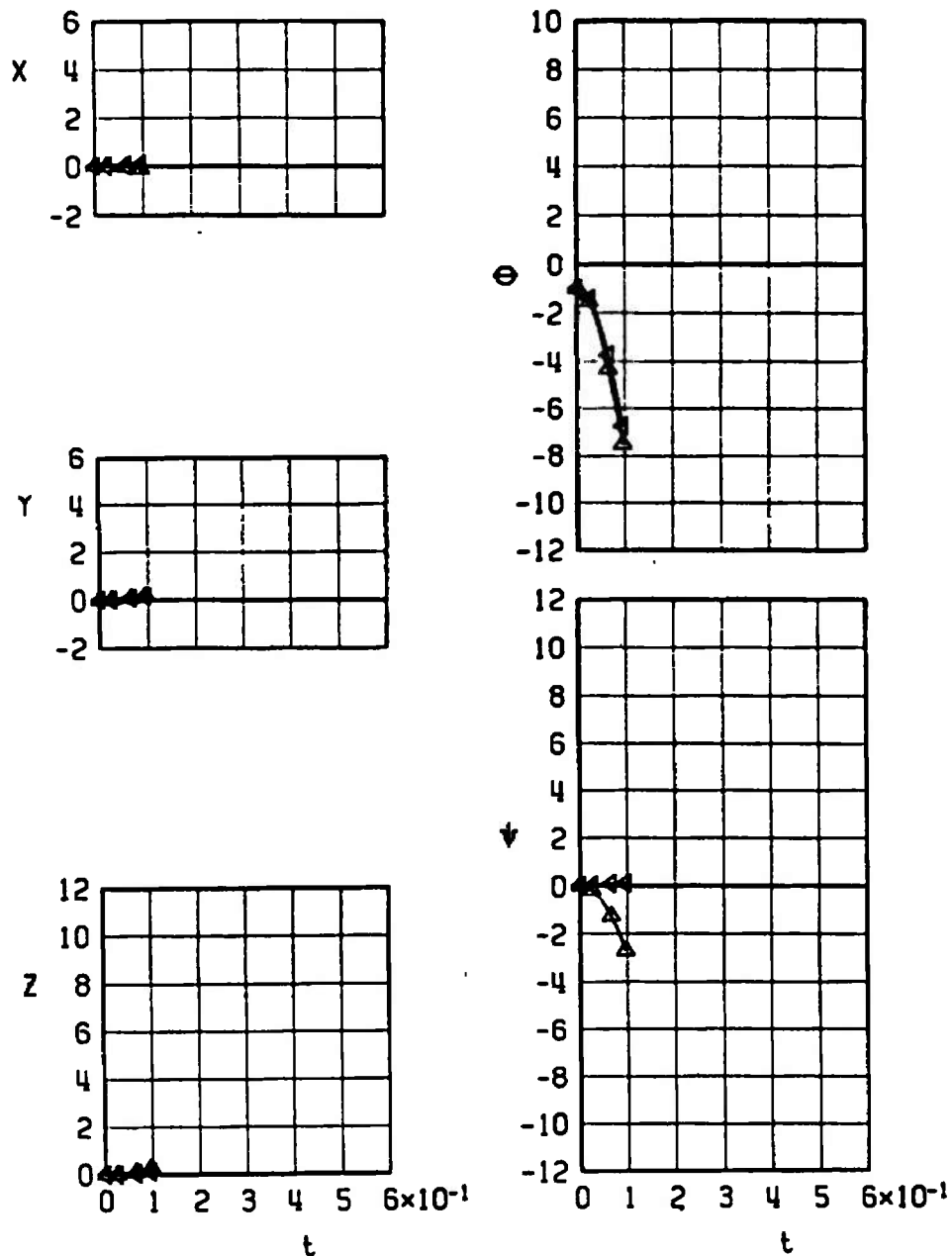
d. Configuration 24L  
Fig. 18 Continued

| SYMBOL          | CONF | $M_\infty$ | $\alpha$ | H    | $\bar{H}$ | EJECTOR FORCE |
|-----------------|------|------------|----------|------|-----------|---------------|
| $\triangleleft$ | 25L  | 0.78       | 2.1      | 7000 | -70       | T1            |
| $\triangle$     | 25L  | 0.95       | 1.9      | 7000 | -70       | T1            |



e. Configuration 25L  
Fig. 18 Continued

| SYMBOL      | CONF | $M_\infty$ | $\alpha$ | H    | $\bar{F}$ | EJECTOR FORCE |
|-------------|------|------------|----------|------|-----------|---------------|
| $\triangle$ | 26L  | 0.78       | 2.1      | 7000 | -70       | T1            |
| $\Delta$    | 26L  | 0.95       | 1.9      | 7000 | -70       | T1            |



f. Configuration 26L  
Fig. 18 Concluded

| SYMBOL | CONF | $M_\infty$ | $\alpha$ | H    | EJECTOR FORCE |
|--------|------|------------|----------|------|---------------|
| ■      | 27R  | 0.33       | 13.1     | 4000 | 0             |
| ○      | 27R  | 0.81       | 3.0      | 4000 | T3            |

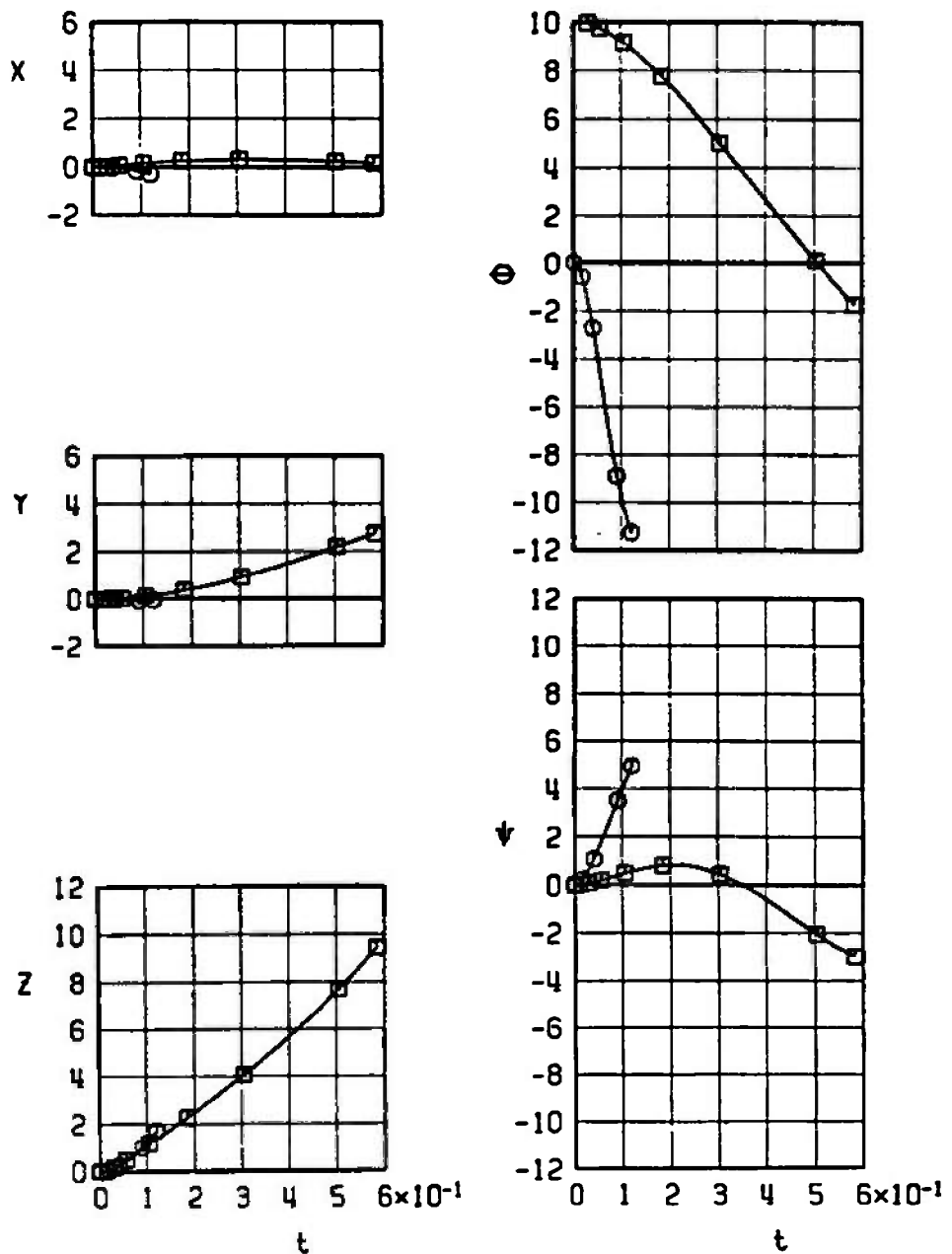


Fig. 19 Effect of Mach Number on the Separation Trajectories of the SUU-42/A from the Outboard Pylon, MER on Center Pylon, and Inboard Pylon Empty, Configuration 27R

| SYMBOL | CONF | $M_\infty$ | $\alpha$ | H    | EJECTOR FORCE |
|--------|------|------------|----------|------|---------------|
| ■      | 28L  | 0.33       | 13.1     | 4000 | 0             |
| ○      | 28L  | 0.81       | 3.0      | 4000 | T3            |

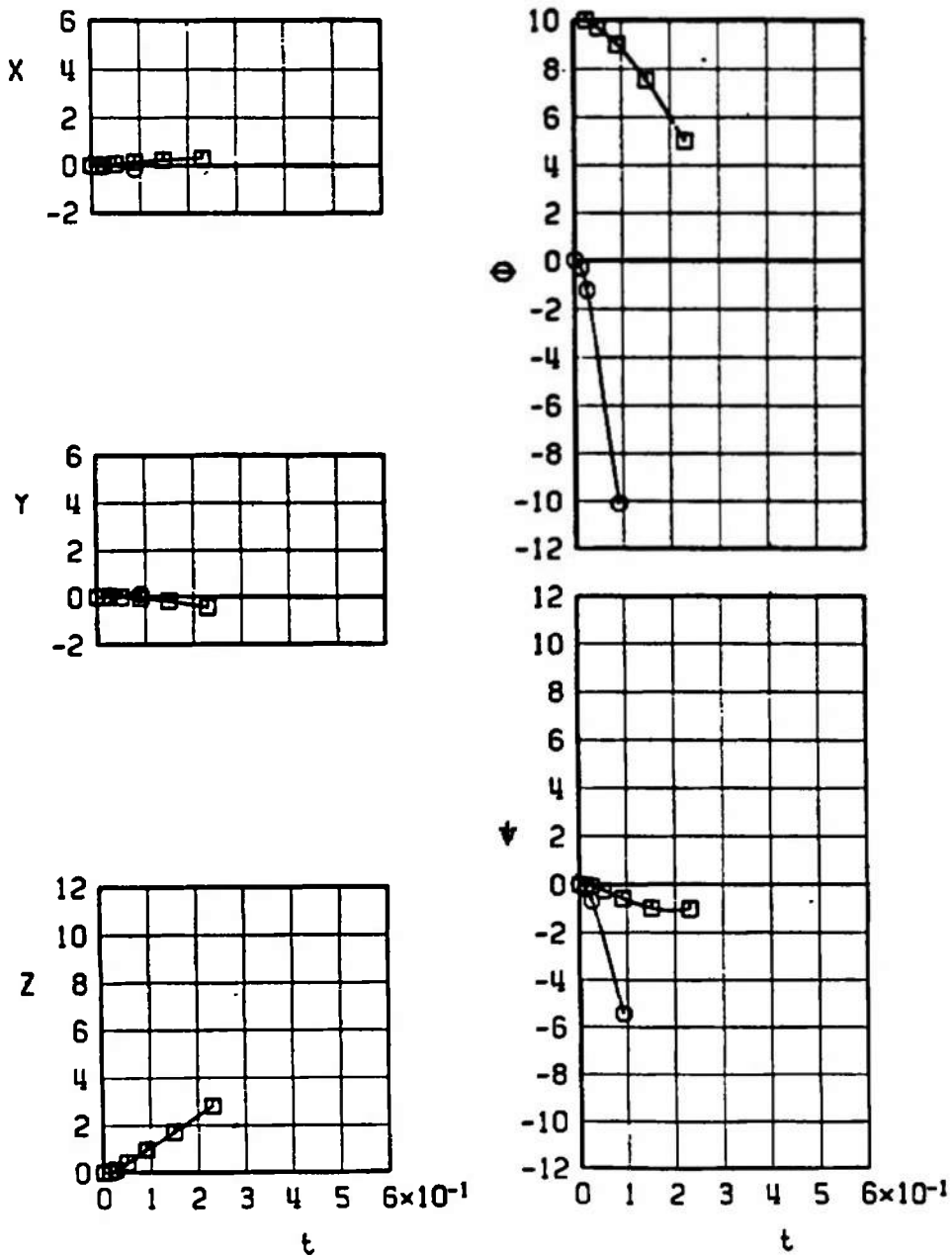
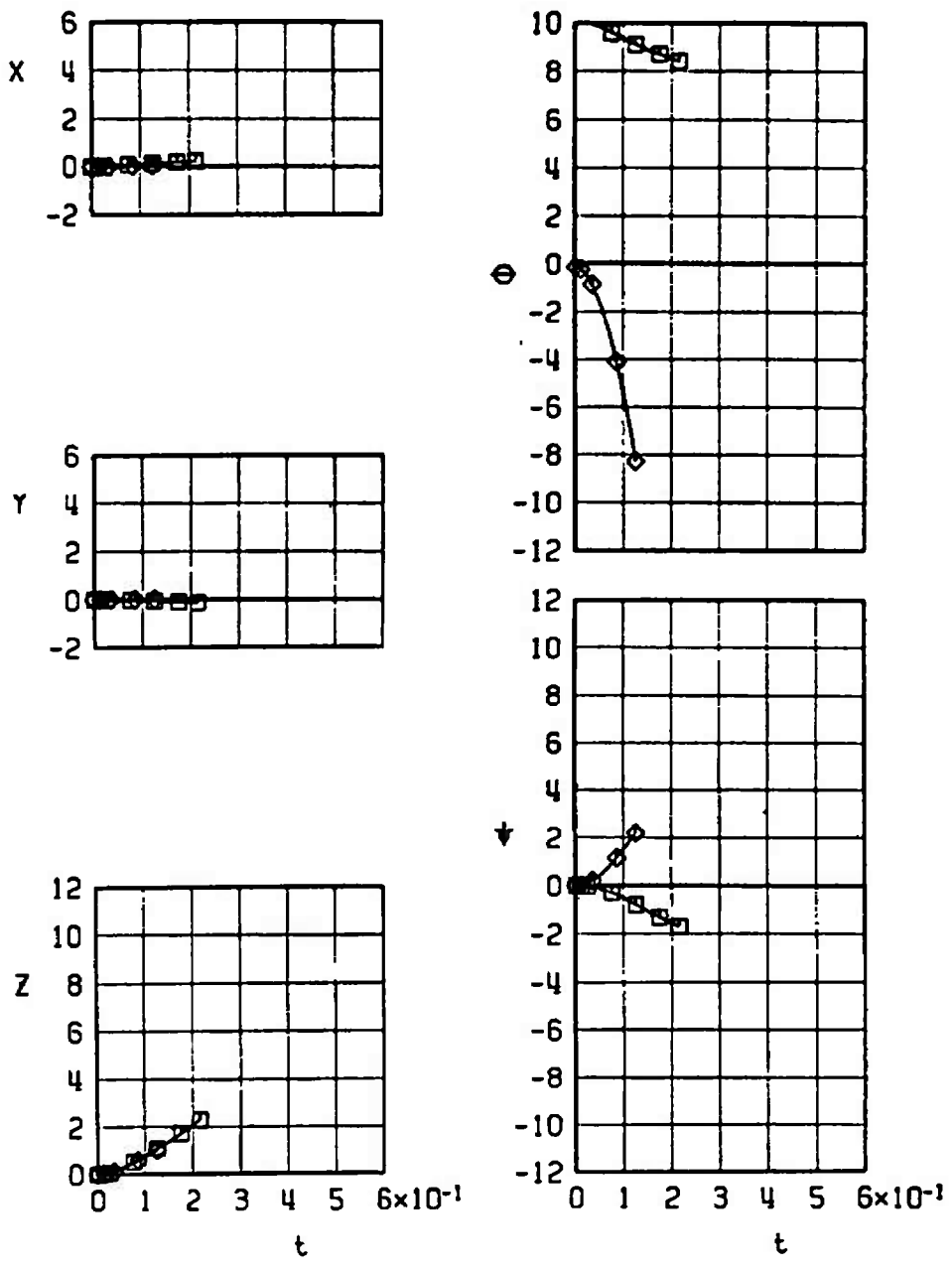


Fig. 20 Effect of Mach Number on the Separation Trajectories of the SUU-42/A from the Outboard Pylon, MER with M-117R on Center Pylon, and an M-117R on Inboard Pylon, Configuration 28L

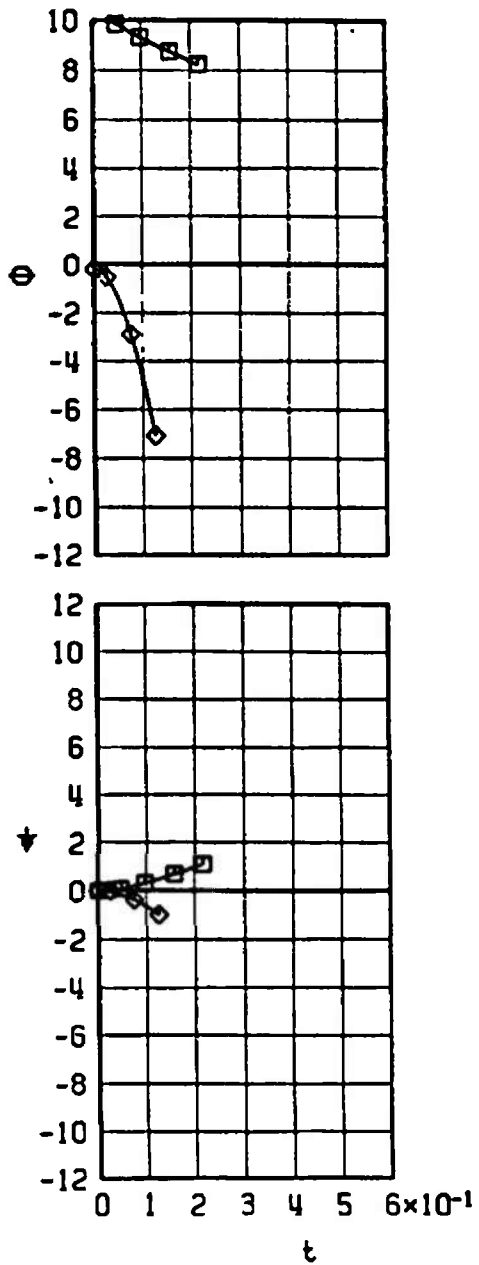
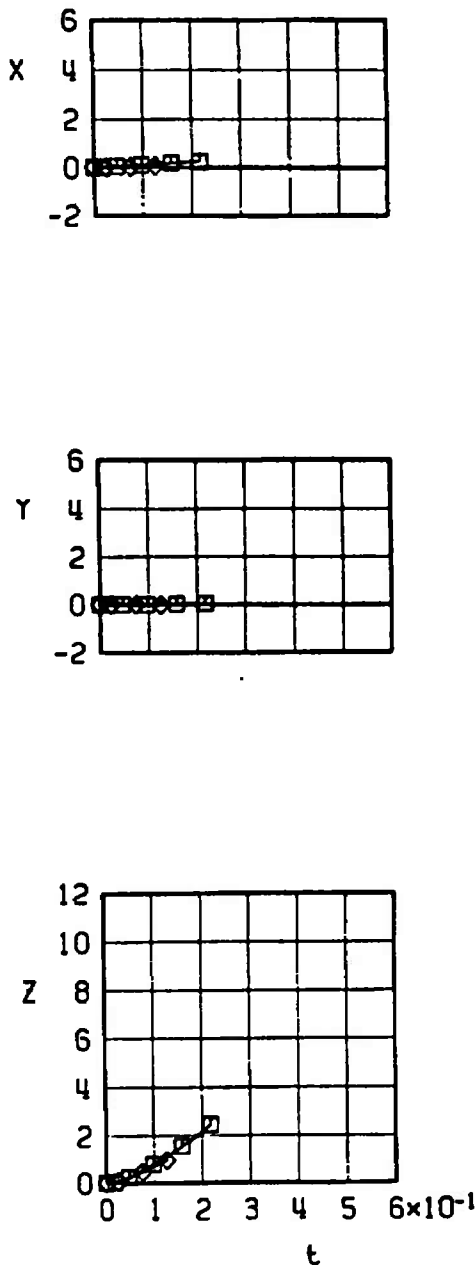
| SYMBOL | CONF | $M_\infty$ | $\alpha$ | H    | $\bar{e}$ | EJECTOR FORCE |
|--------|------|------------|----------|------|-----------|---------------|
| □      | 29L  | 0.33       | 13.1     | 4000 | 0         | T2            |
| ◊      | 29L  | 0.76       | 2.8      | 6000 | -50       | T2            |



a. Configuration 29L

Fig. 21 Effect of Mach Number and Climb Angle on the Separation Trajectories of the Finned BLU-1C/B from the Inboard Pylon, MER on Center Pylon, and Finned BLU-1C/B on Outboard Pylon

| SYMBOL | CONF | $M_\infty$ | $\alpha$ | H    | •   | EJECTOR FORCE |
|--------|------|------------|----------|------|-----|---------------|
| □      | 30R  | 0.33       | 13.1     | 4000 | 0   | T2            |
| ◊      | 30R  | 0.76       | 2.8      | 6000 | -50 | T2            |



b. Configuration 30R  
Fig. 21 Concluded

**TABLE I**  
**FULL-SCALE STORE PARAMETERS USED IN TRAJECTORY CALCULATIONS**

| Parameter   | Store               |        |                     |
|---|---------------------|--------|---------------------|
|   | BLU-1/B<br>(Finned) | M-117R | SUU-42/A<br>(Empty) |
| $\bar{m}$   | 23.00               | 26.90  | 11.90               |
| $X_{cg}$  | 5.45                | 2.80   | 7.08                |
| $I_{yy}$  | 145.00              | 66.90  | 75.50               |
| $I_{zz}$  | 145.00              | 66.90  | 75.50               |
| $b$   | 1.550               | 1.333  | 1.895               |
| $S$   | 1.887               | 1.396  | 2.820               |
| $C_{m_q}$   | -48.0               | -42.0  | -43.4               |
| $C_{n_r}$   | -48.0               | -42.0  | -43.4               |
| Ejector Piston Distance<br>Forward of Store cg,<br>$X_L$ , ft |                     |        |                     |
| 1. $X_L$ , MER or TER   | ---                 | 0.058  | ---                 |
| 2. $X_{L_1}$ , MAU-12   | 0.916               | ---    | 0.666               |
| 3. $X_{L_2}$ , MAU-12   | -0.750              | ---    | -1.000              |
| $Z_E$   | 0.344               | 0.255  | 0.344               |

**TABLE II**  
**MAXIMUM FULL-SCALE POSITION UNCERTAINTIES**  
**CAUSED BY BALANCE INACCURACIES**

| Store                | $M_{\infty}$ | t   | $\Delta X$ | $\Delta Y$ | $\Delta Z$ | $\Delta \theta$ | $\Delta \psi$ |
|----------------------|--------------|-----|------------|------------|------------|-----------------|---------------|
| BLU-1C/B<br>(Finned) | 0.33         | 0.2 | $\pm 0.05$ | $\pm 0.05$ | $\pm 0.06$ | $\pm 0.5$       | $\pm 0.6$     |
| M-117R               | 0.33         | 0.2 | $\pm 0.03$ | $\pm 0.04$ | $\pm 0.01$ | $\pm 0.2$       | $\pm 0.1$     |
| SUU-42/A             | 0.33         | 0.2 | $\pm 0.05$ | $\pm 0.03$ | $\pm 0.02$ | $\pm 0.3$       | $\pm 0.3$     |

**TABLE III**  
**AIRCRAFT WING-LOADING CONFIGURATION**

| Loading Configuration | Launch Store Model | Inboard Pylon           | Center Pylon   | Outboard Pylon          |
|-----------------------|--------------------|-------------------------|--|-------------------------|
| 1L                    | M-117R             | Empty                   | MER: M-117R (Dummy)<br>Sta: 3,4,6<br>M-117R (Launch)<br>Sta: 5 | Empty                   |
| 2L                    | M-117R             | Empty                   | MER: M-117R (Dummy)<br>Sta: 4<br>M-117R (Launch)<br>Sta: 3     | Empty                   |
| 3L                    | M-117R             | Empty                   | MER: M-117R (Launch)<br>Sta: 4                                 | Emoty                   |
| 4L                    | M-117R             | Empty                   | MER: M-117R (Dummy)<br>Sta: 2 - 6<br>M-117R (Launch)<br>Sta: 1 | Empty                   |
| 5L                    | M-117R             | Empty                   | TER: M-117R (Dummy)<br>Sta: 2<br>M-117R (Launch)<br>Sta: 3     | Empty                   |
| 6R                    | M-117R             | Empty                   | TER: M-117R (Launch)<br>Sta: 3                                 | Empty                   |
| 7R                    | M-117R             | Empty                   | TER: M-117R (Dummy)<br>Sta: 2,3<br>M-117R (Launch)<br>Sta: 1   | Empty                   |
| 8R                    | M-117R             | Finned BLU-1C/B (Dummy) | MER: M-117R (Dummy)<br>Sta: 4<br>M-117R (Launch)<br>Sta: 3     | Finned BLU-1C/B (Dummy) |

TABLE III (Continued)

| Loading Configuration | Launch Store Model | Inboard Pylon             | Center Pylon   | Outboard Pylon          |
|-----------------------|--------------------|---------------------------|--|-------------------------|
| 9R                    | M-117R             | Finned BLU-1C/B (Dummy)   | MER: M-117R (Dummy)<br>Sta: 2 ~ 4<br>M-117R (Launch)<br>Sta: 1 | Finned BLU-1C/B (Dummy) |
| 10R                   | M-117R             | Finned BLU-1C/B (Dummy)   | MER: M-117R (Dummy)<br>Sta: 3,4<br>M-117R (Launch)<br>Sta: 2   | Finned BLU-1C/B (Dummy) |
| 11R                   | M-117R             | Finned (BLU-1C/B (Dummy)) | MER: M-117R (Launch)<br>Sta: 4                                 | Finned BLU-1C/B (Dummy) |
| 12R                   | M-117R             | Finned BLU-1C/B (Dummy)   | TER: M-117R (Launch)<br>Sta: 2                                 | Finned BLU-1C/B (Dummy) |
| 13R                   | M-117R             | M-117R (Dummy)            | MER: M-117R (Dummy)<br>Sta: 2 ~ 4<br>M-117R (Launch)<br>Sta: 1 | Empty                   |
| 14R                   | M-117R             | M-117R (Dummy)            | MER: M-117R (Dummy)<br>Sta: 3,4<br>M-117R (Launch)<br>Sta: 2   | Empty                   |
| 15R                   | M-117R             | M-117R (Dummy)            | MER: M-117R (Dummy)<br>Sta: 4<br>M-117R (Launch)<br>Sta: 3     | Empty                   |
| 16R                   | M-117R             | M-117R (Dummy)            | MER: M-117R (Dummy)<br>Sta: 4                                  | Empty                   |

TABLE III (Continued)

| Loading Configuration | Launch Store Model | Inboard Pylon             | Center Pylon   | Outboard Pylon            |
|-----------------------|--------------------|---------------------------|--|---------------------------|
| 17R                   | M-117R             | M-117R (Dummy)            | TER: M-117R (Dummy)<br>Sta: 2<br>M-117R (Launch)<br>Sta: 1     | Empty                     |
| 18R                   | M-117R             | M-117R (Dummy)            | TER: M-117R (Launch)<br>Sta: 2                                 | Empty                     |
| 19L                   | M-117R             | Unfinned BLU-1C/B (Dummy) | MER: M-117R (Dummy)<br>Sta: 6<br>M-117R (Launch)<br>Sta: 5     | Unfinned BLU-1C/B (Dummy) |
| 20L                   | M-117R             | Unfinned BLU-1C/B (Dummy) | TER: M-117R (Launch)<br>Sta: 2                                 | Unfinned BLU-1C/B (Dummy) |
| 21L                   | M-117R             | M-117R (Dummy)            | MER: M-117R (Dummy)<br>Sta: 2 - 4<br>M-117R (Launch)<br>Sta: 1 | SUU-42 (Dummy)            |
| 22L                   | M-117R             | M-117R (Dummy)            | MER: M-117R (Dummy)<br>Sta: 3, 4<br>M-117R (Launch)<br>Sta: 2  | SUU-42 (Dummy)            |
| 23L                   | M-117R             | M-117R (Dummy)            | MER: M-117R (Dummy)<br>Sta: 4<br>M-117R (Launch)<br>Sta: 3     | SUU-42 (Dummy)            |
| 24L                   | M-117R             | M-117R (Dummy)            | MER: M-117R (Launch)<br>Sta: 4                                 | SUU-42 (Dummy)            |

TABLE III (Concluded)

| Loading Configuration | Launch Store Model | Inboard Pylon            | Center Pylon   | Outboard Pylon  |
|-----------------------|--------------------|--------------------------|--|-----------------|
| 25L                   | M-117R             | M-117R (Dummy)           | TER: M-117R (Dummy)<br>Sta: 2<br>M-117R (Launch)<br>Sta: 1 | SUU-42 (Dummy)  |
| 26L                   | M-117R             | M-117R (Dummy)           | TER: M-117R (Launch)<br>Sta: 2                             | SUU-42 (Dummy)  |
| 27L                   | SUU-42             | Empty                    | MER: Empty   | SUU-42 (Launch) |
| 28L                   | SUU-42             | M-117R (Dummy)           | MER: M-117R (Dummy)<br>Sta: 1 - 4                          | SUU-42 (Launch) |
| 29L                   | Finned BLU-1C/B    | Finned BLU-1C/B (Launch) | MER: M-117R (Dummy)<br>Sta: 1 - 4                          | Empty           |
| 30R                   | Finned BLU-1C/B    | Finned BLU-1C/B (Launch) | MER: Empty   | Empty           |

## UNCLASSIFIED

Security Classification

## DOCUMENT CONTROL DATA - R &amp; D

(Security classification of title, body of abstract and indexing annotation must be entered when the overall report is classified)

|   |  |   |
|---|--|---|
| 1. ORIGINATING ACTIVITY (Corporate author)  |  | 2a. REPORT SECURITY CLASSIFICATION<br><b>UNCLASSIFIED</b> |
| Arnold Engineering Development Center<br>Arnold Air Force Station, Tennessee  |  | 2b. GROUP<br><b>N/A</b>                                   |
| 3. REPORT TITLE<br><b>SEPARATION CHARACTERISTICS OF THE M-117 RETARDED BOMB, FINNED BLU-1C/B BOMB, AND SUU-42/A DISPENSER FROM THE A-7D AIRCRAFT AT MACH NUMBERS FROM 0.33 TO 0.95</b>  |  |   |
| 4. DESCRIPTIVE NOTES (Type of report and inclusive dates)<br><b>September 11 through 16, 1971 - Final Report</b>  |  |   |
| 5. AUTHOR(S) (First name, middle initial, last name)<br><b>David W. Hill, Jr., ARO, Inc.</b> This document has been approved for public release by <i>Pey DB 74/17</i><br>its distribution is unlimited. <i>TD 16 August 74</i>   |  |   |
| 6. REPORT DATE<br><b>December 1971</b>  | 7a. TOTAL NO OF PAGES<br><b>67</b>   | 7b. NO. OF REFS<br><b>1</b>                               |
| 8a. CONTRACT OR GRANT NO  | 9a. ORIGINATOR'S REPORT NUMBER(S)  |   |
| b. PROJECT NO.<br><br>c. Program Element 27121F   | <b>AEDC-TR-71-261</b><br><b>AFATL-TR-71-152</b>  |   |
| d. System 337A  | <b>9b. OTHER REPORT NO(S) (Any other numbers that may be assigned this report)</b><br><b>ARO-PWT-TR-71-213</b> |   |
| 10. DISTRIBUTION STATEMENT <b>Distribution limited to U.S. Government agencies only; this report contains information on test and evaluation of military hardware, December 1971; other requests for this document must be referred to Air Force Armament Laboratory (DLGC), Eglin AFB, Florida 32542.</b>  |  |   |
| 11. SUPPLEMENTARY NOTES<br><br><b>Available in DDC</b>  | 12. SPONSORING MILITARY ACTIVITY<br><br><b>AFATL (DLGC)</b><br><b>Eglin AFB, Florida 32542</b>                 |   |
| 13. ABSTRACT <b>Tests were conducted in the Aerodynamic Wind Tunnel (4T) using 0.05-scale models to investigate the separation characteristics of the M-117 retarded bomb, finned BLU-1C/B bomb, and SUU-42/A dispenser when released from various wing pylon locations on the A-7D aircraft. Captive trajectory data were obtained at Mach numbers from 0.33 to 0.95 at simulated pressure altitudes from 4000 to 7000 ft. The parent-aircraft angle of attack was varied from 1.8 to 12.3 depending on Mach number, climb angle, and simulated altitude. At selected test conditions, parent climb angles of -70 deg were simulated. In general, for the trajectory intervals of the test, most of the stores separated from the parent aircraft without store-to-parent contact.</b> |  |   |
| Distribution limited to U.S. Government agencies only; this report contains information on test and evaluation of military hardware; December 1971; other requests for this document must be referred to Air Force Armament Laboratory (BLGC), Eglin AFB, Florida 32542.  |  |   |

**UNCLASSIFIED**

Security Classification

| 14.<br>KEY WORDS  | LINK A |    | LINK B |    | LINK C |    |
|---|--------|----|--------|----|--------|----|
|   | ROLE   | WT | ROLE   | WT | ROLE   | WT |
| separation<br>characteristics<br>M-117 Retarded Bomb<br>BLU-1C/B Bomb (Finned)<br>SUU-42/A Dispenser<br>A-7D Aircraft<br>Mach numbers |        |    |        |    |        |    |